Title
Angular dependence of superconductivity in superconductor / spin valve heterostructures

Author
Jara Abarzua, Alejandro Andres

Publication Date
2017

Peer reviewed|Thesis/dissertation

UNIVERSITY OF CALIFORNIA,
IRVINE

Angular dependence of superconductivity in superconductor / spin valve heterostructures

THESIS

submitted in partial satisfaction of the requirements
for the degree of

MASTER OF SCIENCE

in Chemical and Material Physics

by

Alejandro Andrés Jara Abarzúa

Thesis Committee:
Professor Ilya Krivorotov, Chair
Professor Zuzanna Siwy
Professor Wilson Ho

2017

DEDICATION

To My Parents:
Myriam and Raúl

TABLE OF CONTENTS

LIST OF FIGURES

ACKNOWLEDGMENTS

I would like first to express my gratitude to my research advisor, Professor Ilya Krivorotov. His support and guidance have been crucial to my research. His leadership has allowed to create a unique team of people where each member contributes to keep growing the group and to pass on knowledge to the following generations. I would also like to thank the members of my doctoral committee, Dr. Zuzanna Siwy and Dr. Wilson Ho, for taking time out of their busy schedules to help me accomplish this important task.

I would like to thank everyone who has contributed directly or indirectly to my research. Dr. Brian Youngblood and Dr. Yu-Jin Chen, who were the first people to teach me how to do experiments in the lab. Jian Zhu and Graham Rowlands, who helped me by answering all my questions by e-mail. My coworker Chris Safranski, with whom I published my first paper with professor Ilya Krivorotov's group. Dr. Zheng Duan and Dr. Liu Yang, who guided me through my first steps in the fabrication process. Dr. Andrew Smith and Jen-Ru Chen, for being awesome partners in the fabrication tasks. Dr. Han Kyu Lee and Dr. Eric Montoya, for allowing me to learn from their big research experience. Harmeet Gill and Amanatullah Khan, for giving me the opportunity to teach them and give my first steps as a mentor. Dr. Jieyi Zhang, Chengcen Sha, Josh Dill, Alexandre Goncalves, and Tobias Schneider, although I haven't collaborated with them directly, they have been great labmates. I would also like to give special thanks to Dr. Igor Barsukov for guiding me in different projects and for teaching me concepts of condensed matter. I wanted to thank Dr. Qiyin Lin for teaching me how to do XRD characterization. I would also like to thank my collaborators including professor Oriol Valls, Chien-Te Wu, Abdul N. Malmi-Kakkada, and Klaus Halterman for their great theoretical work in superconducting proximity effect.

Finally, I would like to thank my friends and family. I am deeply indebted to my parents Myriam and Raúl and to my siblings Bárbara and Raúl Jr. for being the pillars of my life. Also, I am wholeheartedly grateful to my partner in all this process, my wife Tracy Dunstan, for her love and emotional support, and to my daughter Emilia Jara who is my source of energy.

I would like to acknowledge Physical Review B. for allowing the use of "Angular dependence of superconductivity in superconductor/spin-valve heterostructures" in chapter 3 of this dissertation.

Funding support from the prestigious Fulbright-CONICYT Scholarship during the first four years of my graduate program is acknowledged.

CURRICULUM VITAE

Alejandro Andrés Jara Abarzúa

EDUCATION

M.S. in Chemical and Material Physics	Physics and Astronomy Department, University of California, Irvine, 2017
M.S. in Physics	Facultad de Ciencias Fisicas y Matematicas, Universidad de chile, 2010
B.S in Physics	Facultad de Ciencias Fisicas y Matematicas, Universidad de chile, 2007

RESEARCH EXPERIENCE

2012-2017	Proximity effects in superconducting/ferromagnetic nanostructures & Nanofabrication and characterization Graduate Research Assistant, Physics and Astronomy Department, University of California, Irvine.
2008-2010	Normal modes in ferromagnetic and dielectric nanowires Graduate Research Assistant, Facultad de Ciencias Fisicas y Matematicas, Universidad de Chile.
July 2007-December 2007	Measuring dislocation density in aluminum with ultrasound spectroscopy Undergraduate Research Assistant, Facultad de Ciencias Fisicas y Matematicas, Universidad de Chile.
January 2007-March 2007	The breakup of a water drop and a glycerin drop Undergraduate Research Assistant, James Franck Institute, University of Chicago.

TEACHING EXPERIENCE

2015 Teaching Assistance
Physics and Astronomy Department,
University of California, Irvine.

2005-2009 Teaching Assistance
Facultad de Ciencias Fisicas y Matematicas,
Universidad de Chile.

RECOGNITION & AWARDS

PhD's degree Scholarship Miguel Velez Scholarship
University of California , 2016

PhD's degree Scholarship US-Chile Equal Opportunities Scholarship
FULBRIGHT-CONICYT , 2011-2015

Master's degree Scholarship Departamento de Fisica Scholarship
universidad de chile, 2008-2009

Bachelor's degree Scholarship Juan Gomez Millas Scholarship
Chilean Ministry of Education, 2003-2007

Academic Excellence Recognition The Highest Score in Mathematics in National University Admission Process, 2002
H. Consejo de Rectores Universidades Chilenas

RESEARCH INTERESTS

- *Experimental Physics, Condensed Matter Physics, Nanomagnetism, Spintronics, Nanofabrication and Characterization, Proximity effects in ferromagnetic/superconducting nanostructures*

PUBLICATION

- *Highly textured IrMn3(111) thin films grown by magnetron sputtering*
  Alejandro Jara, I. Barsukov, B. Youngblood, Y.-J. Chen, J. Read, Hua Chen, P. Braganca, I.N. Krivorotov, IEEE Magn. Lett. **accepted**, (2016).

- *Angular dependence of superconductivity in superconductor/spin-valve heterostructures*
  Alejandro Jara, Christopher Safranski, Ilya N. Krivorotov, Chien-Te Wu, Abdul N. Malmi-Kakkada, Oriol T. Valls, and Klaus Halterman, PHYSICAL REVIEW B **89** 184502 (May 2014).

- *Plasmons and the electromagnetic response of nanowires*
  Alejandro Jara, R.E. Arias and D.L. Mills, PHYSICAL REVIEW B **81** 08542 (FEB 2010).

- *Measuring Dislocation Density in Aluminum with Resonant Ultrasound Spectroscopy*
  Felipe Barra, Andres Caru, Maria Teresa Cerda, Rodrigo Espinoza, Alejandro Jara, Fernando Lund, and Nicolas Mujica, INTERNATIONAL JOURNAL OF BIFURCATION AND CHAOS **19** No. 10 (JAN 2009).

CONTRIBUTED TALKS & POSTERS

January 2016 *"MMM — INTERMAG, 2016 Joint Conference, San Diego"*,
A.A. Jara, I. Barsukov, B. Youngblood, Y. Chen, J.C. Read, P.M. Braganca and I. Krivorotov "Epitaxial growth of IrMn3 thin films by sputter deposition" (Talk)

January 2016 *"MMM — INTERMAG, 2016 Joint Conference, San Diego"*,
C.J. Safranski, I. Barsukov, H. Lee, T. Schneider, A.A. Jara, A. Smith, H. Chang, M. Wu and I. Krivorotov "Spin Current Control of Damping in YIG/Pt Nanowires." (Talk)

January 2016 *"MMM — INTERMAG, 2016 Joint Conference, San Diego"*,
H. Lee, I. Barsukov, C.J. Safranski, A.A. Jara, L. Yang, A. Swartz, B. Kim, H. Hwang and I. Krivorotov "Magnetization dynamics in LSMO/Pt nanowires in the presence of spin Hall torques." (Talk)

March 2015 *"American Physical Society March Meeting, San Antonio, March 2015"*,
Alejandro A. Jara, Igor Barsukov, Yu-Jin Chen, Brian Youngblood, John Read, Patrick Braganca, Ilya Krivorotov "Epitaxial IrMn3 on MgO(111) by sputter deposition" (Talk)

March 2014 *"American Physical Society March Meeting, Denver, March 2014"*,
Alejandro A. Jara, Christopher Safranski, Ilya N. Krivorotov, Chien-Te Wu, Oriol T. Valls "Angular dependence of superconductivity in spin valve / superconductor heterostructures" (Talk)

November 2013 *"58th Conference on Magnetism and Magnetic Materials, Denver"*,
Alejandro A. Jara, Christopher Safranski, Ilya N. Krivorotov, Chien-Te Wu, Oriol T. Valls "Angular dependence of superconductivity in spin valve / superconductor heterostructures" (Talk)

October 2010 *"Escola Brasil-Chile de Nanomagnetismo 2010"*, Instituto de Fisica, Universidade Federal do Rio Grande do Sul Porto Alegre, R.S. - Brasil
Alejandro A. Jara, R.E. Arias, and D.L. Mills "Magnetostatic modes in ferromagnetic nanowires" (Poster)

August 2010 *"II Escuela de Magnetismo"*, University of Santiago of Chile, Santiago, Chile
Alejandro A. Jara, R.E. Arias, and D.L. Mills "Magnetostatic modes in ferromagnetic nanowires" (Poster)

December 2009 *"VI Taller de Jvenes Cientficos iniciativa Cientfica Milenio"*, Santiago, Chile
Alejandro A. Jara, R.E. Arias, and D.L. Mills "Plasmons and the electromagnetic response of dielectric nanowires" (Poster)

June 2009 *"Workshop in Magnetism"*, Club de Campo Coya, Rancagua, Chile
Alejandro A. Jara, R.E. Arias, and D.L. Mills "Plasmons and the electromagnetic response of dielectric nanowires" (Talk)

PROFESSIONAL MEMBERSHIPS

- *American Physical Society (APS).*

ABSTRACT OF THE THESIS

Angular dependence of superconductivity in
superconductor / spin valve heterostructures

By

Alejandro Andrés Jara Abarzúa

Master of Science in Chemical and Material Physics

University of California, Irvine, 2017

Professor Ilya Krivorotov, Chair

This thesis describes a experiment that demonstrates the ability to have magnetic control of the triplet component amplitude in a Nb/Co/Cu/Co/CoO superconducting spin valve. The experiment is done by measuring the superconducting transition temperature, T_c, in the multilayers as a function of the angle α between the magnetic moments of the Co layers. The measurements reveal that $T_c(\alpha)$ is a nonmonotonic function, with a minimum near $\alpha = \pi/2$. The experimental data were compared with numerical self-consistent solutions of the Bogoliubov–de Gennes equations calculated by our collaborators. This thesis shows that experimental data and theoretical evidence agree in relating $T_c(\alpha)$ to enhanced penetration of the triplet component of the condensate into the Co/Cu/Co spin valve in the maximally noncollinear magnetic configuration.

Chapter 1

Introduction

Superconductor/ferromagnetic (S/F) heterostructures have been a focus of intensive research over the past two decades. Apart from their importance for understanding of fundamental physics of the superconducting proximity effect, S/F nanostructures may find applications in low-power cryogenic computing. Competition between superconducting and ferromagnetic ordering in S/F heterostructures can lead to unusual types of magneto-transport effects emerging from the proximity effect at the S/F interfaces. An example of such an effect is non-monotonic angular magnetoresistance (MR) observed in S/F/F spin valves near the superconducting transition temperature T_c. The origin of this non-monotonic MR is the long-range odd triplet component of the condensate, whose amplitude is controlled by the magnetic configuration of the F layers of the spin valve.

In Chapter 2, I will give background theory that is necessary for understanding the physics in my experimental results. I will start with the two theoretical approaches: phenomenological and microscopical. Then I will explain the superconducting proximity effect in the three possible scenarios where a superconductor is in proximity with: a nonmagnetic metal, a fer-

romagnet with collinear magnetization, and a ferromagnet with non-collinear magnetization. Lastly, I will explain briefly what a GMR spin valve is.

In Chapter 3, I describe the experiment which demonstrates the angular dependence of T_c. It describes the sample fabrication, the characterization at normal states, and then the methods to measure the angular dependence of T_c. Next I give a summary of the theoretical description and I compare with the experimental data. At the end of this chapter, I will provide some discussion of the work.

Finally, I present conclusions in Chapter 4.

Chapter 2

Background

Superconductivity phase is one of the states that many metals and alloys can enter below a critical temperature. This is characterized by two effects: zero electrical resistance and perfect diamagnetism. The first effect was discovered by Kamerlingh Onnes in 1911 with the technique of liquefy helium found that mercury has zero electrical resistance below a critical temperature (T_c) of 4.2K. The second effect was discovered by Meissner and Ochsenfeld in 1933. They found that superconductors behave as perfect diamagnets and therefore magnetic flux is completely zero inside of a superconductor. Almost 40 years after the discovery of superconductivity a phenomenological theory was given by Ginzburg and Landau in 1950. They described the superconducting state through a macroscopic wave function which represent a couple of electrons. Then, in 1957 Bardeen, Cooper, and Schrieffer created a microscopic theory of superconductivity. This fascinating quantum-mechanical model is known as BCS Theory. In addition, many other such as London, Josephson, Bogoliubov, Abrikosov, and Andreev made an enormous contribution to have an adequate theoretical picture of conventional superconductivity.

2.1 Phenomenological Theory of superconductivity

2.1.1 Meissner-Ochsenfeld Effect and London Equation

One effect which is a result of the zero electrical resistance is the absence of magnetic flux inside of a superconductor, even in the presence of a external magnetic field. However, Meissner and Ochsenfeld found experimentally that the superconductivity is destroyed in the presence of an applied field higher than a critical magnetic field (H_c) and therefore the magnetic flux can penetrate the entire sample. They also found a reversible transition, it means that the superconducting state and normal state of the sample are in equilibrium at critical magnetic field. This also means that it is equivalent any way to go from the normal state without a external magnetic field to the superconducting state with a small external magnetic field (lower than H_c). For example, first cold down to get the superconducting state and then applied the small magnetic field is equivalent to first applied the small magnetic field and then cold down the sample. The first path is totally explicable with the fact of zero resistivity. However, the second path is unique property for superconducting materials (expulsion of the magnetic field). This is the very known Meissner-Ochsenfeld Effect. The fact that the magnetic flux is zero inside of superconductor implied that $H = -4\pi M$ which is equivalent to say the susceptibility of a superconductor is $\chi = -1/(4\pi)$. This is the reason why a superconductor can be thought as a perfect diamagnet.

In 1961 London proposed an equation to explain the perfect diamagnetism and the Meissner effect of a superconductor.

$$\vec{B} + \lambda_L^2 \vec{\nabla} \times \vec{\nabla} \times \vec{B} = 0$$

where λ_L is known as the London penetration depth and is given by $\sqrt{\frac{mc^2}{4\pi\mu ne^2}}$. With this equation it is possible to infer that the perpendicular component of the magnetic flux is completely vanished at the surface of a superconductor. However, the parallel component decay exponentially into the superconductor in a scale of λ_L.

2.1.2 Ginzburg-Landau (GL) theory

They proposed that the superconductivity is due to a population of superconducting electrons whose density vanishes at the superconducting transition temperature (T_c). They express the density in term of a macroscopic wave function as $n = |\Psi|^2$. Based in the Landau's general theory of second-order phase transformations and the interaction between the vector potential and the wave function, they suggested the free energy to be

$$f = \int \frac{d\vec{r}}{V}\alpha|\Psi|^2 + \frac{\beta}{2}|\Psi^4| + \frac{1}{8\pi}B^2 + \frac{1}{2m^*}\left|\left[\frac{\hbar}{i}\vec{\nabla} + \frac{e^*}{c}\vec{A}(\vec{r})\right]\right|^2 \tag{2.1}$$

where e^* is the effective charge. In 1961 Deaver and Fairbank [1] and Doll and Näbauer [2] discovered experimentally that the effective charge is $2e$. The fact that $e^* = 2e$ suggests that superconductivity is due to a pair of electrons. The minima of the free energy gives the equilibrium states of the system. Minimizing the Ginzburg-Landau free energy independently with respect to the vector potential and the macroscopic wave function gives rise to the

Ginzburg-Landau equations

$$\vec{j}(\vec{r}) = -\frac{2e\hbar}{2im^*}\left[\Psi^*\vec{\nabla}\Psi - \Psi\vec{\nabla}\Psi^*\right] - \frac{4e^2}{m^*c}\vec{A}\Psi^*\Psi \tag{2.2}$$

$$0 = \left[\alpha + \beta|\Psi|^2 + \frac{1}{2m^*}\left(\frac{\hbar}{i}\vec{\nabla} + \frac{e^*}{c}\vec{A}\right)^2\right]\Psi \tag{2.3}$$

with boundary condition

$$\hat{n}\cdot\left(\frac{\hbar}{i}\vec{\nabla} + \frac{e^*}{c}\vec{A}\right)\Psi = 0 \tag{2.4}$$

solving the GL equations is possible to get the London equation and therefore the London penetration depth in terms of GL's parameters as $\lambda_L^2 = \frac{m^*c^2\beta}{4\pi|\alpha|(2e)^2}$. In addition of this length, GL equations depend on the spatial variation of Ψ (order parameter). This length is known as coherence length and is given by $\xi^2 = \frac{\hbar^2}{2m^*|\alpha|}$. The critical field can also be expressed by GL's parameters as $H_c = \sqrt{\frac{4\pi}{\beta}}\alpha$

2.1.3 Type I and II S.C.

The GL theory is very successful to explain the existence of two types of superconductors. In 1957 Abrikosov published a study showing the existence of new type of superconductor which he called Type II. These superconductors have a seconds critical field (H_{c2}) higher than H_c. Therefore, if the sample is below H_c, it is in the superconducting state with the magnetic flux completely expelled from the sample. If the sample is above H_{c2}, it is at normal state and the magnetic flux penetrates completely the sample. Now, if the sample is at a field between H_c and H_{c2}, it will be a mixed state where a superocnductor has some

normal state regions forming vortices where the magnetic field is able to pass through. On the other hand, superconductor type I do not have this second critical field or saying in different way $H_{c2} < H_c$ therefore there is not mixed state because below H_c the sample is completely superconductor. In term of GL's parameters this can be said as

$$\frac{H_{c2}}{H_c} = \sqrt{2}\kappa \tag{2.5}$$

where $\kappa = \lambda/\xi = \frac{m^* c}{e\hbar}\sqrt{\frac{\beta}{8\pi}}$. Then, if $\kappa < 1/\sqrt{2}$ the superconductor is Type I and if $\kappa > 1/\sqrt{2}$ the superconductor is Type II.

2.2 Microscopic Theory of Superconductivity

2.2.1 BCS and Bogoliubov model Hamiltonians

Bardeen, Cooper, and Schrieffer proposed a very successful model of superconductivity. This model consist of pairs of electrons with opposite spins and wave vectors, and therefore with zero center of mass momentum. Latter, in 1958 Bogoliubov proposed a model for a superconductor in a external magnetic field. This model Hamiltonian was a modify version of the BCS model Hamiltonian. Here the center of mass of the pairs of electrons acquire a finite momentum ($\vec{q}$). The BCS and Bogoliubov model Hamiltonians are

$$H_{BCS} = \sum_{\vec{k},\sigma} \epsilon_{\vec{k}} \hat{c}^\dagger_{\vec{k}\sigma} \hat{c}_{\vec{k}\sigma} + \sum_{\vec{k}\vec{k}'} U_{\vec{k}\vec{k}'} \hat{c}^\dagger_{\vec{k}\uparrow} \hat{c}^\dagger_{-\vec{k}\downarrow} \hat{c}_{-\vec{k}'\downarrow} \hat{c}_{\vec{k}'\uparrow} \tag{2.6}$$

$$H_{Bogoliubov} = \sum_{\vec{k}\vec{k}'\sigma} \epsilon_{\vec{k}\vec{k}'} \hat{c}^\dagger_{\vec{k}\sigma} \hat{c}_{\vec{k}\sigma} - \sum_{\vec{k}\vec{q}\vec{k}'} \frac{U_0}{V} \hat{c}^\dagger_{\vec{k}\uparrow} \hat{c}^\dagger_{\vec{q}-\vec{k}\downarrow} \hat{c}_{\vec{q}-\vec{k}'\downarrow} \hat{c}_{\vec{k}'\uparrow} \tag{2.7}$$

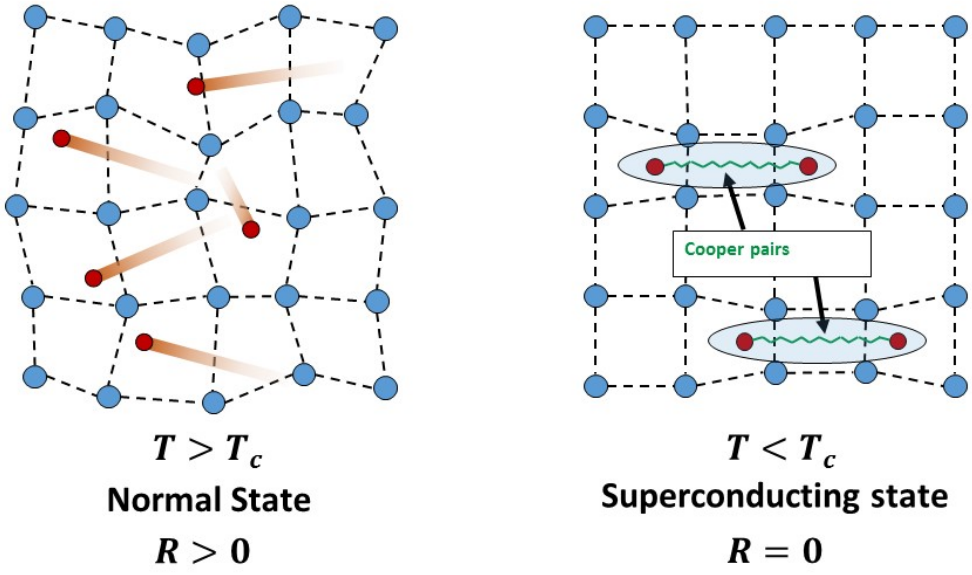

Figure 2.1: Schematic of atoms and electrons of a metal in the Normal and superconducting state

these hamiltonians describe the dynamics of a pair of electrons. This pair is known as Cooper pair because Cooper was the first person to show that a small attractive interaction between electrons in a metal can bind electrons into pairs.

2.2.2 Cooper pair

The concept of Cooper pair presented in this thesis is for conventional superconductor such as Nb and Ta. This excludes other kind of superconductivity like High-Temperature superconductor. Figure 2.1 shows a schematic representation of the interaction between a lattice of atoms of a metal (blue circles) with its conduction electrons (red circles). If this metal is at a temperature higher than the critical temperature, it behaves like a normal metal. So its conduction electrons encounter resistance, which is caused by collisions and scattering as the particles move through the vibrating lattice of metal atoms. Instead, at low temperature below a critical temperature, the lattice of atom has coordinated movements with the con-

duction electrons. This interaction between the electron and the movement of the lattice, known as electron-phonon interaction, creates a small attraction among the electrons. This small attraction is enough to make the electrons condensate in pairs (Cooper pair) and move freely through the metal without resistance.

Cooper pair as a quantum mechanic system is described by a wavefunction. In principle, there are four spin states for a electron pair: $\uparrow\uparrow$, $\downarrow\downarrow$, $\uparrow\downarrow$, and $\downarrow\uparrow$. However, the total wavefunction of a system of two electrons has to be antisymmetric or odd with respect to exchange of the two electrons. The wavefunction can be separated in two parts.

$$\Psi(r_1, s_1; r_2, s_2) = \psi(r_1; r_2)S(s_1, s_2) \tag{2.8}$$

$\psi(r_1; r_2)$ is the orbital part which describe the distribution of the particles in the space and $S(s_1, s_2)$ is the spin part which describe the spin of the particles of the system. In order to have odd wavefunction, one of the parts has to be odd and the other even. Therefore, we have two possibilities: one where the spin part if even and the other where the spin part is odd. In the case of the spin part is even, we have three possible function which are even: $\uparrow\uparrow$, $\downarrow\downarrow$, $\uparrow\downarrow + \downarrow\uparrow$. These three components are called triplet. In the case of the spin part is odd, there is only one possible wavefunction which is odd or antisymmetric: $\uparrow\downarrow - \downarrow\uparrow$. This is called singlet. In principle all these four component could be present in a superconductor. However, in a conventional superconductor the orbital part is symmetric (s-wave), then only the singlet condensation is present. In other words, superconducting correlations in conventional superconductors form Cooper pairs with anti-aligned spins.

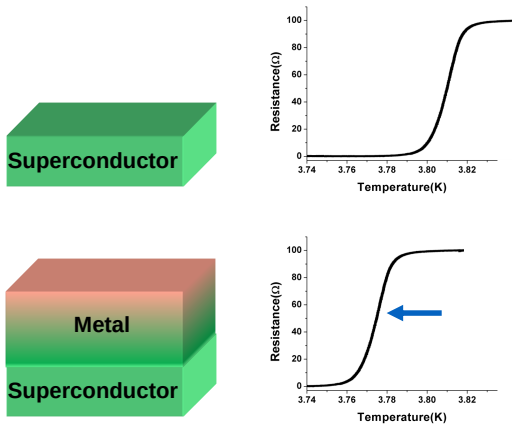

Figure 2.2: Representation of how the penetration of the Cooper pair can change the superconducting transition temperature

2.3 Superconducting Proximity Effect

The superconducting proximity effect is the key concept of this work. It has been studied intensively because in proximity structures was possible to see some effects which were not observed in bulk materials. Figure 2.2 shows a phenomenological description of the proximity effect. This schematic representation is relevant for understanding the experimental procedure and results. Figure 2.2(a) shows the representation of a superconductor thin film and its superconducting transition temperature curve, then if there is a metal in proximity, the superconducting transition temperature decrease, Fig 2.2(b). The reason is that there is penetration of the condensate into the non-superconducting layer. Then, part of the non-superconducting layer becomes superconducting by proximity. The price of this transformation is that the whole structure has a lower superconducting transition temperature. So, in simple words, more penetration of the condensate, lower superconducting transition temperature.

Penetration of the condensate depends on the characteristic of the metal such as thickness or the magnetic properties. The proximity effect between a conventional superconductor and

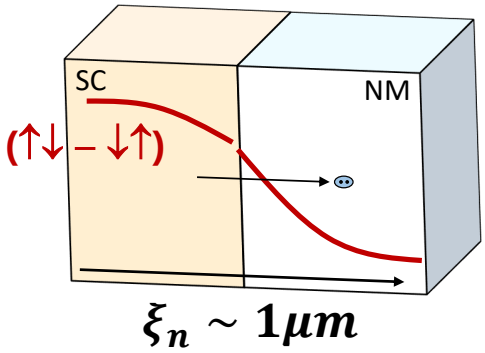

Figure 2.3: Superconducting proximity effect between a conventional superconductor and a nonmagnetic metal

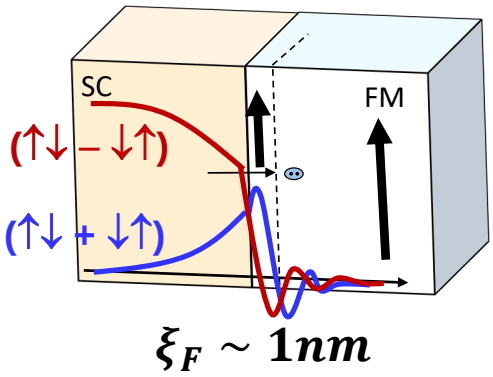

Figure 2.4: Superconducting proximity effect between a conventional superconductor and a ferromagnetic metal with collinear magnetization

a nonmagnetic metal (fig.2.3), the singlet Cooper pair amplitude decays monotonically into the nonmagnetic metal in a long range of the order of 1μm.

If the nonmagnetic metal is replaced by ferromagnetic metal, the scenario is quiet different. Superconducting correlations in conventional superconductor form Cooper pairs with anti-aligned spins, while the exchange interaction in the ferromagnetic metals tends to align the spins of the conduction electrons which produce the pair breaking. As a result of the competing interactions, the Cooper pair can not penetrate deep into the ferromagnet. In other words, the proximity effect induces short range state of the order of 1 nm.

However, this is not the end of the story, the real situation is much more complex and interesting. When there are magnetization collinearities (fig.2.4), each electron of the singlet Cooper pair acquire a different momentum due to the exchange splitting of the conduction band in the ferromagnet layer. Then, the Cooper pair have a finite momentum which produces a change in the amplitude of the cooper pair. By using the Eulers formula, the pair wavefunction can be rewritten as a mixture of singlet and triplet spin states with zero spin projection.

$$(\uparrow\downarrow - \downarrow\uparrow) \rightarrow (\uparrow\downarrow e^{iQ\cdot R} - \downarrow\uparrow e^{-iQ\cdot R}) \tag{2.9}$$

$$\rightarrow (\uparrow\downarrow - \downarrow\uparrow)\mathrm{Cos}(\mathrm{Q}\cdot\mathrm{R}) + i(\uparrow\downarrow + \downarrow\uparrow)\mathrm{Sin}(\mathrm{Q}\cdot\mathrm{R}) \tag{2.10}$$

The new state has a oscillatory behavior in space inside of the ferromagnet. The state is known as FFLO state. It was predicted by Peter Fulde and Richard Ferrell and by Anatoly Larkin and Yurii Ovchinnikov. The S/F proximity effect has an important consequence inducing singlet to Triplet conversion process.

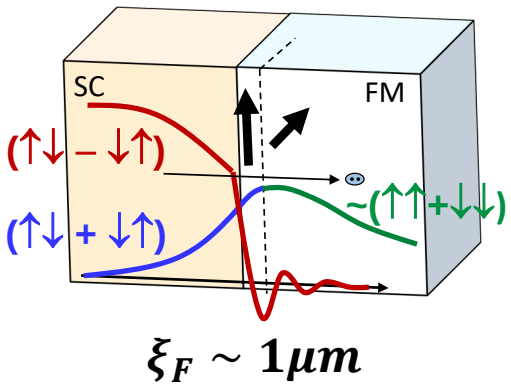

Figure 2.5: Superconducting proximity effect between a conventional superconductor and a ferromagnetic metal with noncollinear magnetization

The amplitude of this proximity-induced triplet state depends on the state of magnetization of the ferromagnet. When there are magnetization noncollinearities (fig.2.5), the proximity effect induces all three components of the triplet condensate. Because there is no preferred quantization axis (and neither the total spin S of the Cooper pairs nor its z-component are conserved). The components with parallel spins are immune to pair breaking by the exchange field and, they can penetrate deep into the ferromagnet and give rise to the long-range triplet component in the ferromagnet of the order of 1μm.

2.4 GMR

A spin-valve (SV) is a magnetic structure which consists of two ferromagnetic thin layers separated by a nonmagnetic layer which avoid the direct exchange coupling between the ferromagnetic layers. The resistance of a SV depends on the relative orientation of the magnetizations of the two ferromagnets.

For example, two magnetic configuration of the SV is the parallel and the antiparallel configuration. Figure fig.2.6 show a schematic of these two states. These configurations have

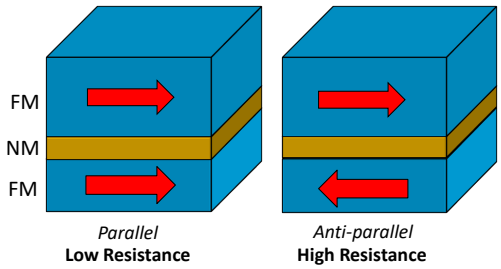

Figure 2.6: Schematic of the parallel and antiparallel configurations of a SV

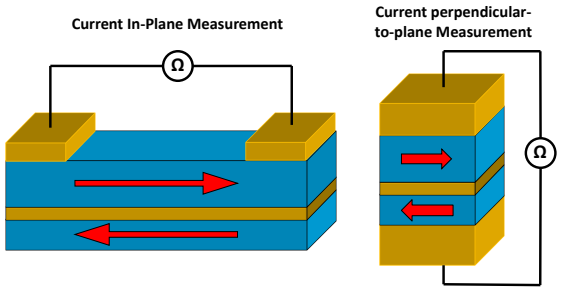

Figure 2.7: Current in plane and current-perpendicular-to-plane configurations of a SV

different resistance, the parallel configuration has lower resistance than the antiparallel one. This effect is known as Giant Magnetoresistance (GMR) and it was discovered independently by Albert Fert and Peter Grunberg in 1988. Then, they received the Nobel Prize in Physics in 2007 for their work. It was an important discovery for the development of compact hard disks used, for example, in computers and some music players.

There are two methods to measure the GMR effect by performing current in plane (CIP) measurement or by performing current perpendicular-to-plane (CPP)measurement, 2.7. In this thesis, the measurements were performed using CIP. There are some advantages of the CIP measurement on thin-film multilayers. First, it is much easier to fabricate the samples than for CPP and therefore we could make and study many sample with different thicknesses. Second, it is convenient to compare with theoretical description due to the translational symmetry in the multilayer plane.

Bibliography

[1] Bascom S. Deaver and William M. Fairbank. "Experimental Evidence for Quantized Flux in Superconducting Cylinders". In: *Phys. Rev. Lett.* 7 (2 1961), pp. 43–46. URL: https://link.aps.org/doi/10.1103/PhysRevLett.7.43.

[2] R. Doll and M. Näbauer. "Experimental Proof of Magnetic Flux Quantization in a Superconducting Ring". In: *Phys. Rev. Lett.* 7 (2 1961), pp. 51–52. URL: https://link.aps.org/doi/10.1103/PhysRevLett.7.51.

Chapter 3

Angular dependence of superconductivity in superconductor / spin valve heterostructures

The contents of this chapter are adapted from work originally published as *Phys. Rev. B 89, 184502 (2014)*. This is a collaborative work between an experimental group at UC Irvine leading by professor Ilya Krivorotov and a theoretical group at the University of Minnesota, Minneapolis leading by professor Oriol Valls.

3.1 Introduction

Competition between superconducting (S) and ferromagnetic (F) ordering in S/F heterostructures can lead to unusual types of superconductivity emerging from the proximity effect at the S/F interfaces [3–11]. Penetration of spin-singlet Cooper pairs from the S into the F material can result, when more than one magnetic orientation is present, in mixing of the

spin-triplet and spin-singlet states by the exchange field and generation of a spin-triplet component of the condensate [8, 9, 12–17]. The amplitude of this proximity-induced triplet state sensitively depends on the state of magnetization of the F material. In particular, the triplet components with nonzero projection of the spin angular momentum of the Cooper pair ($S_z = \pm 1$) can only occur when there are magnetization noncollinearities. These components of the condensate are immune to pair breaking by the exchange field and, unlike the singlet and the $S_z = 0$ triplet components, they can penetrate deep into the F material [9, 17, 18]. This long-range triplet condensate can be manipulated via changing the relative orientation of the magnetizations, which creates opportunities for the development of a new class of superconducting spintronic devices. Recent progress in this direction is demonstration of Josephson junctions with noncollinear magnetic barriers, in which the supercurrent is carried by the long-range triplet component of the condensate [19–21].

Thin-film multilayers of S and F materials are a convenient experimental platform for studies of the proximity-induced triplet condensate [22–30]. The advantages of the F/S multilayers include (i) well-established methods of the multilayer deposition, (ii) easy and controllable manipulation of the magnetic state of the F layers via application of external magnetic field, and (iii) convenience of theoretical description of the condensate owing to the translational symmetry in the multilayer plane. Here we present studies of the dependence of T_c in CoO/Co/Cu/Co/Nb multilayers on the in-plane angle α between the magnetic moments of the Co layers. We compare our experimental results to numerical solutions of the Bogoliubov–de Gennes equations and find that excellent quantitative agreement with the experiment can be achieved when scattering at the multilayer interfaces is taken into account. This solution also reveals that T_c suppression observed for the orthogonal state of the Co magnetic moments originates from enhanced penetration of the long-range triplet condensate into the Co/Cu/Co spin valve in this maximally non-collinear magnetic state. Comparison between the theoretical and experimental $T_c(\alpha)$ allows us to quantify the induced triplet pair amplitude in the spin valve, which reaches values greater than 1% of the singlet pair

amplitude in the Nb layer for the maximally noncollinear ($\alpha = \pi/2$) configuration of the spin valve.

3.2 Sample Preparation and Characterization

The CoO(2 nm)/ Co(d_p)/ Cu(d_n)/ Co(d_f)/ Nb(17 nm)/ (substrate) multilayers, schematically shown in Fig. 3.1(a), were prepared by magnetron sputtering in a vacuum system with a base pressure of 8.0×10^{-9} Torr. The deposition was performed onto thermally oxidized Si substrates at room temperature under an Ar pressure of 2 mTorr. The 2 nm thick CoO layer was formed by oxidation of the top part of the Co layer in air for at least 24 hours. The native CoO film is antiferromagnetic at cryogenic temperatures and its purpose is to pin the direction of the top Co layer via the exchange bias phenomenon [31]. Three series of multilayers, each series with varying thickness of one of the layers (pinned d_p, free d_f, and nonmagnetic d_n) were deposited in continuous runs with minimal breaks between the samples within the series. This ensured that samples within each of the series were prepared in similar residual gas environments. The three multilayer series reported in this work were designed to elucidate the dependence of the triplet condensate pair amplitude on the spin valve parameters. The description of the series geometries is as follows:

Series 1: CoO(2 nm)/ Co(2.5 nm)/ Cu(6 nm)/ Co(d_f)/ Nb(17 nm) with d_f ranging from 0.5 nm to 1.0 nm

Series 2: CoO(2 nm)/ Co(2.5 nm)/ Cu(d_n)/ Co(0.6 nm)/ Nb(17 nm) with d_n ranging from 4 nm to 6.8 nm

Series 3: CoO(2 nm)/ Co(d_p)/ Cu(6 nm)/ Co(0.6 nm)/ Nb(17 nm) with d_p ranging from 1.5 nm to 5.5 nm.

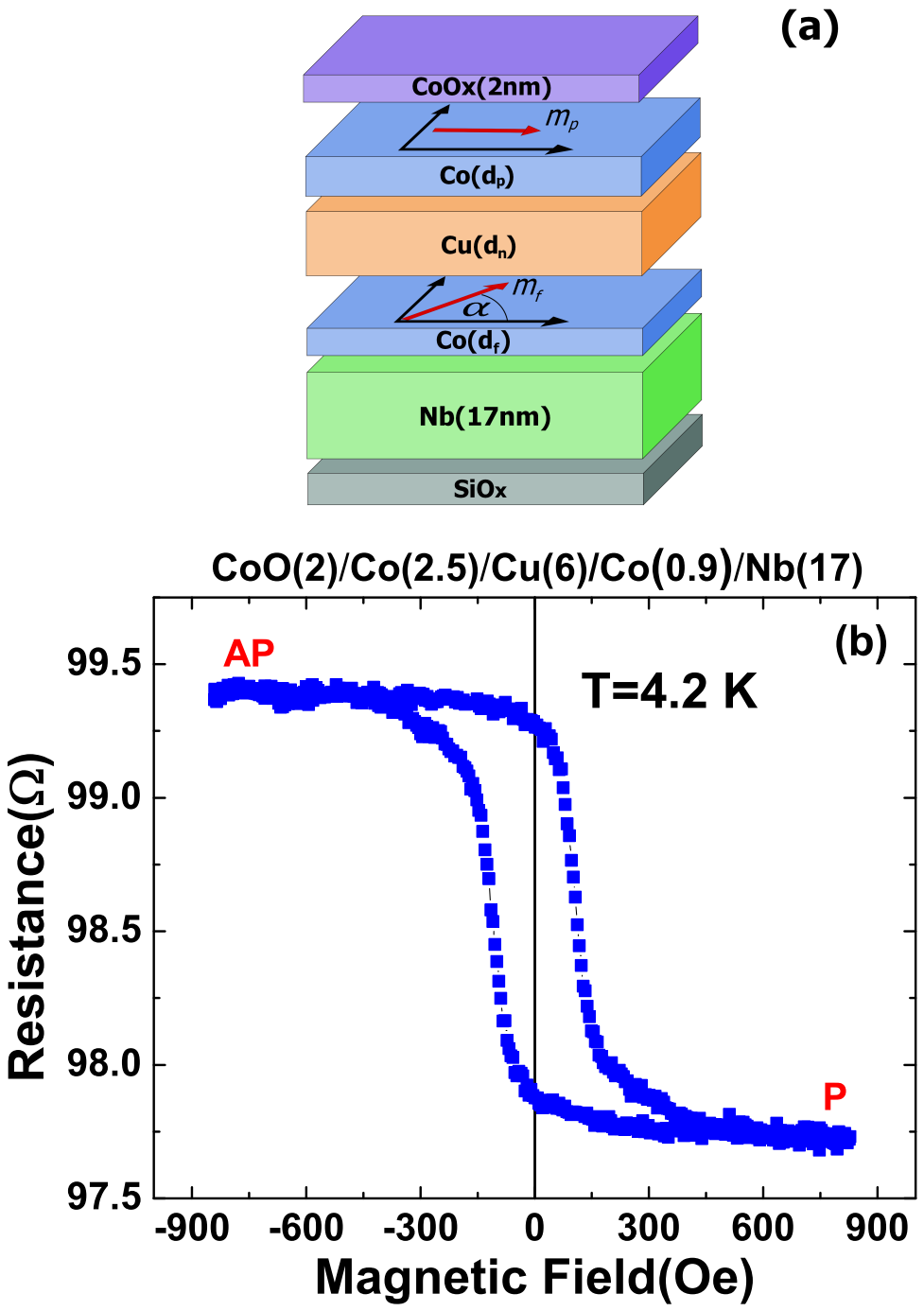

Figure 3.1: (a) Schematic of the CoO(2 nm)/ Co(d_p)/ Cu(d_n)/ Co(d_f)/ Nb(17 nm) multilayer, where α is the in-plane angle between the magnetic moments of the Co layers. (b) Resistance versus the in-plane magnetic field applied parallel to the pinned layer magnetization at $T = 4.2$ K (above the superconducting transition temperature).

The multilayers were patterned into 200 μm-wide Hall bars using photolithography and liftoff. Four-point resistance measurements of the samples were performed in a continuous flow ^{4}He cryostat. The magnetization direction of the top Co layer was pinned in the plane of the sample by a strong ($\sim$ 1 T) [31] exchange bias field from the antiferromagnetic CoO layer. The exchange bias field direction was set by a 1500 Oe in-plane magnetic field applied to the sample during cooling from the room temperature. As we demonstrate below, the magnetization of the free Co layer can be easily rotated in the plane of the sample by a relatively small ($\sim$ 500 Oe) magnetic field. The role of the nonmagnetic Cu spacer layer is to decouple the magnetic moments of the Co layers, and it is chosen to be thick enough (d_n >4 nm) so that both the direct and the RKKY [32] exchange interactions between the Co layer are negligibly small. In all magnetoresistance measurements reported here, care is taken to align the applied magnetic field with the plane of the sample so that vortex flow resistance is negligible [33].

Figure 3.1(b) shows the resistance of a CoO(2 nm)/ Co(2.5 nm)/ Cu(6 nm)/ Co(0.9 nm)/ Nb(17 nm) sample as a function of the magnetic field applied along the exchange bias direction measured at T = 4.2 K (above the superconducting transition temperature T_c). At T = 4.2 K, all samples show the conventional giant magnetoresistance (GMR) effect originating from the Co/Cu/Co spin valve. Given that there is significant current shunting through the Nb layer, the magnitude of the GMR ($\sim$2%) is large, demonstrating good quality of both Co/Cu interfaces [32]. The GMR curve also demonstrates that external in-plane magnetic field of $\geq$ 500 Oe fully saturates the free layer magnetization along the applied field direction. The lack of an offset in the GMR hysteresis loop from the origin demonstrates that the interlayer exchange coupling between the Co layers is negligible.

3.3 Angular Dependence of T_c

We next make measurements of the multilayer superconducting transition temperature T_c as a function of the angle α between magnetic moments of the pinned and free layers. We define T_c as the temperature at which the sample resistance becomes equal to half of its normal state value. For these measurements, we use an 800 Oe in-plane magnetic field to set the direction of magnetization of the free layer. As discussed in the previous section, this field completely saturates the magnetization of the free layer in the direction of the field. Furthermore, this field is much smaller than the exchange bias field acting on the pinned layer and thus we assume that the pinned layer magnetization remains in the direction of the cooling field for all our measurements. Figure 3.2 shows resistance versus temperature measured in the parallel (P, $\alpha = 0$), antiparallel (AP, $\alpha = \pi$), and perpendicular (90°, $\alpha = \pi/2$) configurations of the two Co layers for the samples with 0.5 nm and 1.0 nm thick Co free layers, and 2.5 nm thick Co pinned layer. In this measurement, the angle between the magnetic moments is pinned by the in-plane external field while the temperature is swept across the superconducting transition. To ensure that the sample remains in thermal equilibrium with the bath, the temperature for each measurement is swept at a sufficiently slow rate of 2 mK per minute. For both values of the free layer thickness, we find that the perpendicular configuration of the spin valve ($\alpha = \pi/2$) gives the lowest transition temperature T_c. We find this to be universally true for all samples studied in this work: $T_c(\pi/2) < T_c(0)$ and $T_c(\pi/2) < T_c(\pi)$. In contrast, the relation between T_c in the P and AP configurations depends on the thickness of the free layer. Figure 3.2 shows that $T_c(0) < T_c(\pi)$ for $d_f = 0.5$ nm, while $T_c(\pi) < T_c(0)$ for $d_f = 1.0$ nm. Similar trends in the angular and thickness dependence of T_c were recently observed in Pb/ Fe/ Cu/ Fe/ CoO multilayers [25].

To understand the angular dependence of T_c in greater detail, we fix the temperature in the middle of the superconducting transition and measure the sample resistance R as a function of in-plane angle α between the magnetic moments of the pinned and free layers.

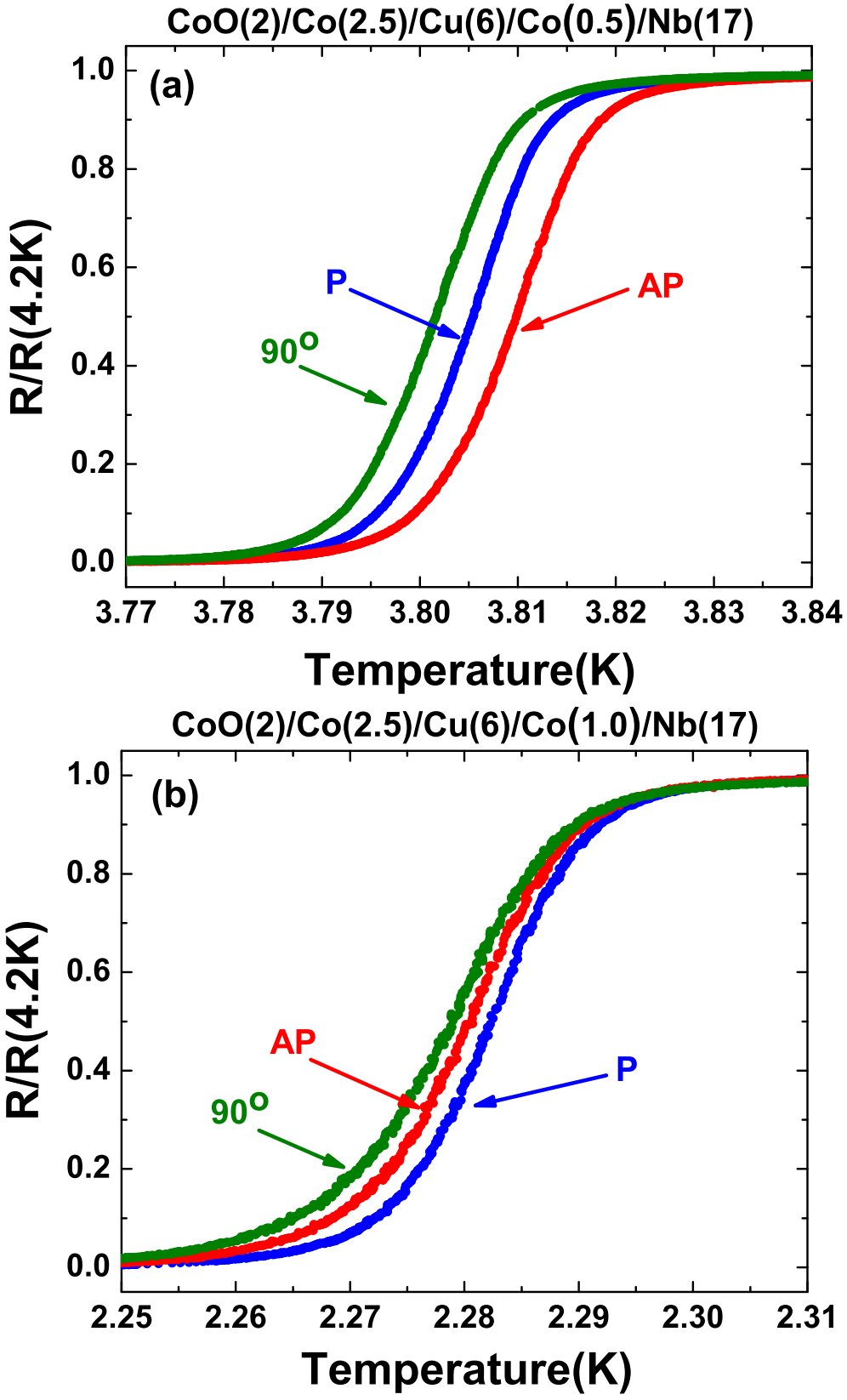

Figure 3.2: Resistance versus temperature for parallel (P, $\alpha = 0$), antiparallel (AP, $\alpha = \pi$), and perpendicular (90°, $\alpha = \frac{\pi}{2}$) orientations of magnetic moments of the Co layers for multilayer samples with (a) $d_f = 0.5$ nm and (b) $d_f = 1.0$ nm. The resistance is divided by its normal state value measured at $T = 4.2$ K.

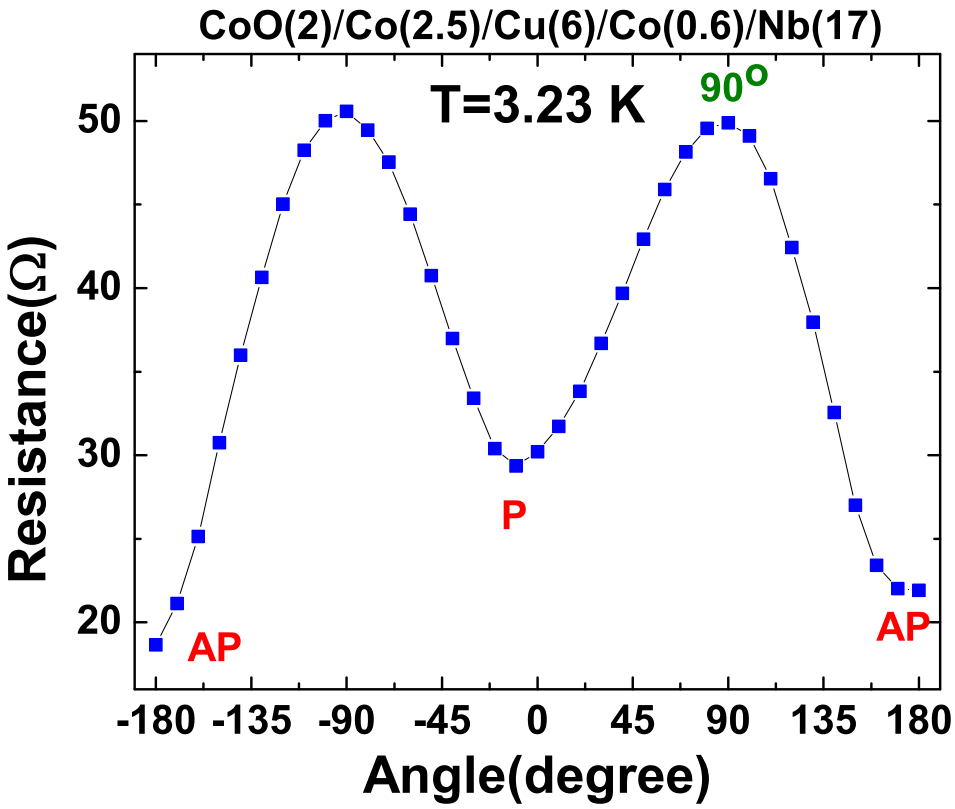

Figure 3.3: Resistance of a CoO(2 nm)/ Co(2.5 nm)/ Cu(6 nm)/ Co(0.6 nm)/ Nb(17 nm) structure versus magnetic field angle, α , measured at $T = 2.92$ K in the middle of the superconducting transition, at a field of 800 Oe.

This measurement is made by applying an 800 Oe saturating magnetic field and rotating it through 360° in the plane of the sample. Figure 3.3 shows $R(\alpha)$ measured at $T = 2.92$ K (the middle of the superconducting transition) for a CoO(2 nm)/ Co(2.5 nm)/ Cu(6 nm)/ Co(0.6 nm)/ Nb(17 nm) sample. Because resistance is a steep function of temperature in the middle of the superconducting transition, we take great care to stabilize the temperature to within ±0.1 mK during these measurements in order to reduce the level of thermal noise in the $R(\alpha)$ data.

Measurements of $R(\alpha)$ are much faster than those of $R(T)$ because reliable $R(T)$ data require sweeping temperature at slow rates. Thus we employ the $R(\alpha)$ data in order to evaluate $T_c(\alpha)$ instead of direct measurements of $T_c(\alpha)$ at multiple values of α, such as those shown in Fig. 3.2. We therefore need a reliable method of extracting $T_c(\alpha)$ from the $R(\alpha)$ data.

The simplest method for such extraction is to use the slope of the $R(T)$ curve at T_c for $\alpha = 0$ and to calculate $T_c(\alpha)$ as $T_c(\alpha) = T_c(0) - (dT/dR)\,[R(\alpha) - R(0)]$, where $R(\alpha)$ is the experimentally measured angular dependence of resistance at $T = T_c(0)$. This simple method assumes approximately linear variation of resistance with temperature near T_c and already gives qualitatively satisfactory results. However, the maximum uncertainty in the resulting $T_c(\alpha)$ can be as large as 5 mK. The purple dotted curve in Fig. (3.4) shows $T_c(\alpha)$ calculated by this method for a CoO(2 nm)/ Co(2.5 nm)/ Cu(6 nm)/ Co(0.6 nm)/ Nb(17 nm) multilayer.

In order to take into account deviations of $R(T)$ from a linear function and thereby improve the procedure for extracting $T_c(\alpha)$ from the $R(\alpha)$ data, we calculate $T_c(\alpha)$ based on the experimentally measured $R(T, 0)$ and $R(T^*, \alpha)$ curves, where $T^* \approx T_c(0)$ is the temperature at which the angular dependence of resistance is measured. In this method, we assume that the shape of the $R(T)$ curve is the same for all values of α, and that the curves at different α can be obtained by simply translating the experimentally measured $R(T, 0)$ curve along the temperature axis by $\Delta T_c(\alpha) = T_c(\alpha) - T_c(0)$. With this assumption, $T_c(\alpha) = T_c(0) + \Delta T_c(\alpha)$ can be found by numerically solving the implicit equation $R(T^*, \alpha) = R(T^* - \Delta T_c(\alpha), 0)$ for $\Delta T_c(\alpha)$. The blue squares in Fig. (3.4) show $T_c(\alpha)$ evaluated by this method using the transition curve from the P ($\alpha = 0$) state. The red triangles and green dots represent the same method used with the other two measured curves. We find this method of evaluating $T_c(\alpha)$ to be quite reliable for our samples with an estimated error of ~ 1 mK.

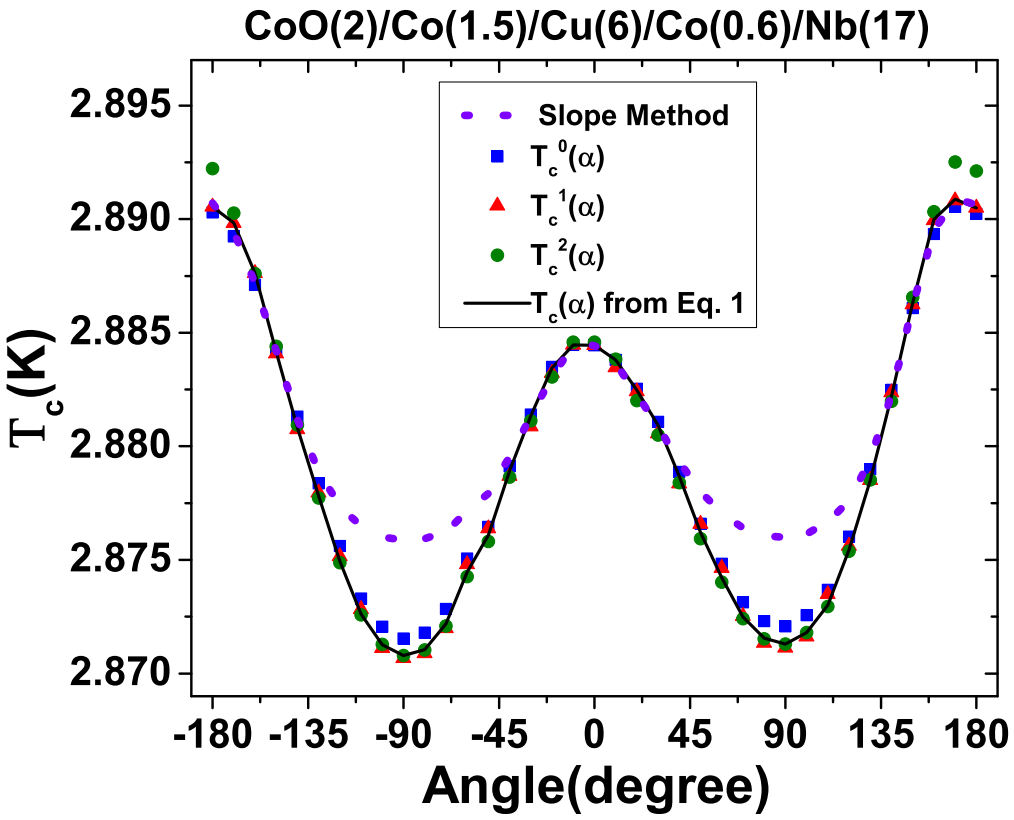

Figure 3.4: $T_c(\alpha)$ for a CoO(2 nm)/ Co(1.5 nm)/ Cu(6 nm)/ Co(0.6 nm)/ Nb(17 nm) multilayer calculated from the $R(\alpha)$ data by different methods described in the text.

An even more refined method of evaluating $T_c(\alpha)$ takes into account that the shape of the $R(T)$ curve (not only its position along the temperature axis) may depend on α. Here we first calculate $\Delta T_c(\alpha)$ based on the experimentally measured $R\,(T, \pi/2)$ and $R(T, \pi)$ curves using the method described above: we calculate $T_c(\alpha)$ by numerically solving the implicit equations $R(T^*, \alpha) = R\,(T^* - \Delta T_c(\alpha), n\pi/2)$ for $\Delta T_c(\alpha)$, where $\Delta T_c(\alpha) = T_c(\alpha) - T_c\,(n\pi/2)$, $n = 1, 2$. These $T_c(\alpha)$ values calculated for $n = 1, 2$ are shown in Fig. (3.4) as green circles and red triangles, respectively. Figure (3.4) clearly illustrates that all three functions $T_c(\alpha)$ calculated by numerically solving the implicit equations written above for $n = 0, 1, 2$ are very similar to each other. The average of these three functions $T_c^n(\alpha)$, which we now explicitly label by the index $n = 0, 1, 2$, would give a reasonable result for $T_c(\alpha)$. However, a better

estimate is given by the following equation:

$$T_c(\alpha) = \sum_{n=0}^{2} T_c^n(\alpha) w_n(\alpha) \tag{3.1}$$

where $w_n(\alpha)$ are extrapolation functions with maxima at $\alpha = \pm n\pi/2$. The extrapolation functions also satisfy the normalization condition $\sum_{n=0}^{2} w_n(\alpha) = 1$ on the interval of α from $-\pi$ to π. We make the following choice of the extrapolation functions: $w_0(\alpha) = \cos^2(\alpha)\Theta\left(\pi/2 - |\alpha|\right)$, $w_1(\alpha) = \sin^2(\alpha)$ and $w_2(\alpha) = \cos^2(\alpha)\Theta\left(|\alpha| - \pi/2\right)$, where $\Theta(x)$ is the Heaviside step function. The advantage of Eq. (3.1) over the simple average is that at $\alpha = 0, \pi/2, \pi$, the expression for $T_c(\alpha)$ reduces to the exact value of T_c directly measured at these angles in the $R(T)$ measurements. The black solid line in Fig. (3.4) shows $T_c(\alpha)$ evaluated by this method. We use this method for calculating $T_c(\alpha)$ from the experimental data throughout the rest of the paper.

Figure 3.5 shows a representative angular variation of T_c, $\Delta T_c(\alpha) = T_c(\alpha) - T_c(0)$, for the three series of samples employed in our study. We find that for all samples employed in our experiment, $T_c(\alpha)$ is a nonmonotonic function in the interval of α from $-\pi$ to π with a minimum near perpendicular orientation of the free and pinned layers ($\alpha = \pi/2$). As we demonstrate in the analysis section of this paper, this minimum in T_c arises from the enhanced long-range triplet pair amplitude in the maximally noncollinear configuration of the spin valve. We also note that our previous studies of the angular dependence of T_c in NiFe/Nb/NiFe trilayers [34] found monotonic dependence of T_c on α in the 0 to π range, which serves as indication of a much weaker triplet pair amplitude induced in the system with two ferromagnetic layer separated by a superconductor.

Figure 3.6 summarizes the dependence of $T_c(\alpha)$ on the thickness of the Co/Cu/Co spin valve layers. Figure 3.6(a) shows the difference of T_c in the P and AP states as a function of the free layer thickness d_f. The data demonstrate that $T_c(\pi) - T_c(0)$ oscillates and changes

sign as a function of d_f, which is a consequence of interference of the pair wave function in the free layer. Figures 3.6(b) and 3.6(c) show the dependence of $T_c(\pi) - T_c(0)$ on the nonmagnetic spacer thickness d_n and the pinned layer thickness d_p. This dependence is weak, which implies that (i) the pair amplitude decays slowly in the Cu spacer layer and (ii) the pair amplitude decays to nearly zero over the pinned layer thickness greater than 1.5 nm (the thinnest pinned layer employed in our studies). The behavior of T_c will be discussed in general later in this work.

Figure 3.6 also illustrates the thickness dependence of T_c in the maximally noncollinear geometry of $\alpha = \pi/2$. The green squares in Fig. 3.6 show the dependence of $T_c(\pi/2) - T_c(0)$ on the spin valve layer thicknesses. This figure clearly shows that $T_c(\pi/2)$ is always lower than $T_c(0)$ and $T_c(\pi)$. Figure 3.6(c) illustrates that $T_c(\pi/2)$ shows variation with the pinned layer thickness for d_p as large as 3.5 nm. This serves as evidence of the long-range (> 3.5 nm) penetration of the triplet component of the condensate into the pinned ferromagnetic layer.

3.4 Theoretical Methods

The theoretical method we adopted is thoroughly discussed in Refs. [11, 17, 35]; therefore, we only present here the essential parts that are necessary for our discussion. In particular, the theoretical method we used to find T_c can be found in Refs. [34, 35]. We modeled the Nb/Co/Cu/Co heterostructures as $S/F_f/N/F_p$ layered systems, where S represents the superconducting layer, F_f and F_p are the inner (free) and outer (pinned) magnets, and N denotes the normal metallic intermediate layer. The layers are assumed to be infinite in the x-z plane with a total thickness d in the y direction, which is perpendicular to the interfaces between layers. In accordance with the experiment, F_p has width d_p, and fixed direction of magnetization. The normal layer with width d_n is sandwiched between this pinned layer and

a magnetic layer $\mathrm{F_f}$ of width d_f with experimentally controlled magnetization direction. The superconducting layer of thickness d_S is in contact with the free layer. The in-plane magnetizations in the F layers are modeled by effective Stoner-type exchange fields $\mathbf{h}(y)$ which vanish in the nonferromagnetic layers. To accurately describe the physical properties of our systems with sizes in the nanometer scale and moderate exchange fields, where semiclassical approximations are inappropriate, we numerically solve the microscopic Bogoliubov–de Gennes (BdG) equations in a fully self-consistent manner. The geometry of our system allows one to express the BdG equations in a quasi-one-dimensional form (natural units $\hbar = k_B = 1$ are assumed),

$$\begin{pmatrix} \mathcal{H}_0 - h_z(y) & -h_x(y) & 0 & \Delta(y) \\ -h_x(y) & \mathcal{H}_0 + h_z(y) & \Delta(y) & 0 \\ 0 & \Delta(y) & -(\mathcal{H}_0 - h_z(y)) & -h_x(y) \\ \Delta(y) & 0 & -h_x(y) & -(\mathcal{H}_0 + h_z(y)) \end{pmatrix} \begin{pmatrix} u_{n\uparrow}(y) \\ u_{n\downarrow}(y) \\ v_{n\uparrow}(y) \\ v_{n\downarrow}(y) \end{pmatrix} = \epsilon_n \begin{pmatrix} u_{n\uparrow}(y) \\ u_{n\downarrow}(y) \\ v_{n\uparrow}(y) \\ v_{n\downarrow}(y) \end{pmatrix}, \tag{3.2}$$

where $h_i(y)$ $(i = x, z)$ are components of the exchange fields $\mathbf{h}(y)$. In Eq. (3.2), the single-particle Hamiltonian $\mathcal{H}_0 = -1/(2m)d^2/dy^2 - E_F + U(y)$ contains the Fermi energy, E_F, and an effective interfacial scattering potential described by delta functions of strength H_j (j denotes the different interfaces); namely,

$$\begin{aligned} U(y) =& H_1\delta(y - d_S) + H_2\delta(y - d_S - d_f) \\ &+ H_3\delta(y - d_S - d_f - d_n), \end{aligned} \tag{3.3}$$

where $H_j = k_F H_{Bj}/m$ is written in terms of the dimensionless scattering strength H_{Bj}. We assume $h_x(y) = h_0 \sin(-\alpha/2)$ and $h_z(y) = h_0 \cos(-\alpha/2)$ in $\mathrm{F_f}$, where h_0 is the magnitude of exchange field. In $\mathrm{F_p}$, we have $h_x(y) = h_0 \sin(\alpha/2)$ and [18] $h_z(y) = h_0 \cos(\alpha/2)$. The functions $u_{n\sigma}$ and $v_{n\sigma}$ ($\sigma =\uparrow, \downarrow$) in Eq. (3.2) represent quasiparticle and quasihole wave

functions. By applying the generalized Bogoliubov transformations (see Ref. [17]), the self-consistent singlet pair potential $\Delta(y)$ can be expressed in terms of quasiparticle and quasihole wave functions; that is,

$$\Delta(y) = \frac{g(y)}{2}\sum_{n}{}' \left[u_{n\uparrow}(y)v_{n\downarrow}(y) + u_{n\downarrow}(y)v_{n\uparrow}(y)\right] \tanh\Big(\frac{\epsilon_n}{2T}\Big), \tag{3.4}$$

where the primed sum means summing over all eigenstates with energies ϵ_n that lie within a characteristic Debye energy ω_D, and $g(y)$ is the superconducting coupling strength, taken to be constant in the S region and zero elsewhere. We have assumed that the quantization axis lies along the z direction, but one can easily obtain the spin-dependent quasiparticle amplitudes with respect to a different spin quantization axis rotated by an angle θ in the x-z plane via the rotation matrix [17]:

$$\hat{U_0}(\theta) = \cos(\theta/2)\hat{\mathrm{I}} \otimes \hat{\mathrm{I}} - i\sin(\theta/2)\rho_z \otimes \sigma_z, \tag{3.5}$$

where $\boldsymbol{\rho}$ and $\boldsymbol{\sigma}$ are vectors of Pauli matrices in particle-hole and spin space, respectively.

In principle, one can obtain the superconducting transition temperatures by computing the temperature dependence of $\Delta(y)$ and identifying the critical temperature where $\Delta(y)$ vanishes. However, the property that the pair potential is vanishingly small near T_c permits one to linearize the self-consistency condition, that is, to rewrite it near T_c in the form

$$\Delta_i = \sum_q J_{iq}\Delta_q, \tag{3.6}$$

where the Δ_i are expansion coefficients in a given basis and the J_{iq} are the appropriate matrix elements with respect to the same basis. To determine T_c, one can simply compare the largest eigenvalue, λ, of the matrix J with unity at a given temperature. The system is in the superconducting state when λ is greater than unity. More details of this efficient technique are discussed in Refs. [34, 35].

To analyze the correlation between the behavior of the superconducting transition temperatures and the existence of odd triplet superconducting correlations in our systems, we compute the induced triplet pairing amplitudes which we denote as f_0 (with $m = 0$ spin projection) and f_1 with ($m = \pm 1$) according to the equations [16, 17]

$$f_0(y,t) = \frac{1}{2}\sum_n \left[u_{n\uparrow}(y)v_{n\downarrow}(y) - u_{n\downarrow}(y)v_{n\uparrow}(y)\right]\zeta_n(t), \tag{3.7a}$$

$$f_1(y,t) = \frac{1}{2}\sum_n \left[u_{n\uparrow}(y)v_{n\uparrow}(y) + u_{n\downarrow}(y)v_{n\downarrow}(y)\right]\zeta_n(t), \tag{3.7b}$$

where $\zeta_n(t) \equiv \cos(\epsilon_n t) - i\sin(\epsilon_n t)\tanh(\epsilon_n/(2T))$. These triplet pair amplitudes are odd in time t and vanish at $t = 0$, in accordance with the Pauli exclusion principle.

3.5 Analysis

In this subsection, we present our theoretical analysis and compare the theoretical results with the experimental data. To find the theoretical T_c, we adopted the linearization method as discussed in Sec. 3.4. The fitting process is rather time-consuming since for every parameter set, one must evaluate T_c numerically as a function of the misalignment angle α, making a least-squares fit unfeasible. The same situation occurs in Refs. [34, 36]. As in those works, we search within plausible regions of parameter space, and display here results of the best fit that we have found, which is not necessarily the best possible fit. There are a number of parameters at one's disposal and, when computing the theoretical values of T_c, we first have to keep the number of fitting parameters as small as possible. All of the relevant physical parameters that are related to the properties of the materials involved, such as the exchange field, and the effective superconducting coherence length, are required to be the same for all of the different samples when performing the fitting. However, for parameters that are affected by the fabrication processes such as the interfacial barrier strength, one can reasonably assume, as we do, that their values are somewhat different from sample to

sample. We do find that the variation is small between different samples in each series. For the material parameters we have found that the best value of the effective Fermi wave vector is $k_F = 1\mathring{A}^{-1}$ and the effective superconducting coherence length $\xi_0 = 11.5\,\mathrm{nm}$. For the dimensionless exchange field $I \equiv h_0/E_F$ (normalized to Fermi energy), we have used, for Co, $I = 0.145$, which is consistent with previous work [17] ($I = 1$ corresponds to the half-metallic limit). For the superconducting transition temperature for a putative pure superconducting sample of the same quality as the material in the layers, we have used $T_c^0 = 4.5$ K. This is the same value previously found [34]. It is of course lower than the true bulk transition temperature of Nb but even for pure thin films a decrease in T_c is to be expected. All of these parameters are kept invariant across all of the different samples, as mentioned earlier. Only the three interfacial barrier strengths are treated as adjustable from sample to sample during the fitting process. We assume, however, that the barrier strength is the same on both sides of the normal metal layer while that between the free ferromagnetic layer and the superconductor are weaker. For each series, the barrier varies somewhat from batch to batch.

They are found to be as follows: $H_{B1} = 0.2$, and both H_{B2} and H_{B3} vary from 0.64 to 0.7 for different batches in the d_f series. For the d_p series, we have $H_{B1} = 0.15$, $0.53 < H_{B2}$, and $H_{B3} < 0.58$. The d_n series have H_{B1} ranges from 0.3 to 0.45 and $H_{B1} = H_{B2} = 0.62$. The thicknesses of the different layers are taken of course from their experimental values. As in Ref. [36] we find a thin magnetic "dead layer" between the normal metal and the free ferromagnetic layer of a small thickness in the range $0.27\,\mathrm{nm} \sim 0.35\,\mathrm{nm}$.

We now compare the experimental and theoretical values of T_c as a function of layer thicknesses and angle α for three different batches of samples: in one we vary d_f, in the second, d_n, and in the last, d_p. First, in Fig. 3.7, we present comparisons between experiment and theory, for the T_c results in the parallel state ($\alpha = 0$) as a function of thickness for the three different series mentioned above. In all three series, the experimental and theoretical T_c are

in very good agreement with each other. For the d_f series, one should notice that both experimental and theoretical T_c are very sensitive to the thicknesses of the free layers. When the thickness of the free ferromagnetic layer is increased, T_c decreases nonmonotonically by almost 50%. However, the d_n and d_p series do not show the same sensitivity, even though the ranges of thicknesses for these two series are much larger compared to that of the d_f series. This lower sensitivity is physically reasonable for the following reason: because of the presence of ferromagnets, we find that the magnitude of the singlet pairing amplitude decreases very fast beyond the boundary, in non-S regions away from the F/S interface. The exchange field reduces the proximity effect. Therefore, the size effects from the thicknesses of normal metal layers and pinned ferromagnetic layers are less. We also observe the trend that both theoretical and experimental T_c are often found to be a nonmonotonic function of the thicknesses of the F layers. In fact, except for the experimental T_c for d_f series, which does not show a clear oscillatory behavior, all other series clearly exhibit the nonmonotonicity of T_c. Oscillatory behavior of transition temperatures as one varies the thickness is standard in hybrid S/F heterostructures due to the oscillatory character of the pair amplitude [37] itself. The reason for the exception found might be that the data points are too widely spaced. This nonmonotonic behavior has been noted in past works [38, 39] and is often found [18] in FFS trilayers.

In Fig. 3.8, we present a detailed comparison of theoretical and experimental results for ΔT_c as a function of angle α between the magnetizations in the free and pinned layers for the d_f, d_n, and d_p series. Each panel in the first row in Fig. 3.8 represents different samples for d_f series. Results for the d_n and d_p series are plotted in the second and third row, respectively. One can clearly see that the behavior of the highly nonmonotonic angular dependencies of the theoretical results presented here describe very well the experimental results, not only qualitatively but also quantitatively: the magnitudes of the experimental and theoretical results for ΔT_c are comparable; both experimental and theoretical results indicate the switching effects are in about the 25 mK range. It is well worth recalling than

in another recent work [34] results for the magnitude of this quantity differed by more than one order of magnitude. In contrast, here, taking into account the existence of numerical and experimental uncertainties (the former we estimate at ~ 1.5 mK), we find theory and experiment in very good agreement. This great improvement over Ref. [34] follows from the more careful treatment of the interface barriers from sample to sample and a much more extensive search in parameter space. For the d_f series, we see that the switching range for both experimental and theoretical $T_c(\alpha)$ varies nonmonotonically when d_f is increased. This occurs for the same reason already mentioned in the discussion of Fig. 3.7: the behavior of $T_c(\alpha)$ is very sensitive to the inner ferromagnetic layer thicknesses due to the proximity effect. Similarly, we observe that the switching ranges are less sensitive to the thickness of the outer ferromagnetic layer (see in the d_p series) and also to the normal metal layer thickness in the d_n series.

We now turn to the role that induced triplet correlations in the nonmonotonic behavior of $T_c(\alpha)$. This has been the subject of recent theoretical interest [18, 40, 41] but little has been done on quantitatively comparing theory and experiment. To examine this question in a quantitative way, we have computed the induced odd triplet pairing correlations. These correlations (as well of course as the ordinary singlet correlations) can be self-consistently calculated using the methods previously described. As noted in Sec. 3.4, with the presence of nonhomogeneous magnetization the triplet pair amplitudes in general can be induced when $t \neq 0$. We present our study in terms of the quantity

$$F_t(y,t) \equiv \sqrt{|f_0(y,t)|^2 + |f_1(y,t)|^2}, \tag{3.8}$$

where the quantities involved are defined in Eq. (3.7). This quantity accounts for both triplet components, the equal spin and opposite spin triplet correlations. The reason to use this quantity is that via Eq. (3.5), one can easily show that, when the spin quantization axis is rotated by an angle θ, the rotated triplet pair amplitudes $\tilde{f}_0$ and $\tilde{f}_1$ after the transformation

are related from the original f_0 and f_1 by

$$\tilde{f}_0(y,t) = \cos(\theta) f_0(y,t) - \sin(\theta) f_1(y,t), \tag{3.9a}$$

$$\tilde{f}_1(y,t) = \sin(\theta) f_0(y,t) + \cos(\theta) f_1(y,t). \tag{3.9b}$$

Therefore the quantity $F_t(y,t)$ that we focus on obviates any ambiguity issues related to the existence of generally non-collinear "natural" axes of quantization in the system.

We have computed this quantity as a function of position and α. It turns out to be particularly useful to focus on the average value of $F_t(y,t)$ in the pinned layer $\mathrm{F_p}$. We normalize this averaged quantity, computed in the low-T limit, to the value of the singlet pair amplitude in the bulk S. This normalized averaged quantity is plotted as a function of α in Fig. 3.9 (left vertical scale) at a dimensionless characteristic time $\omega_D t = 4.0$. This time value is unimportant, provided it be nonzero, of course. In the three panels, an example taken from each of the series is displayed, as explained in the caption. One can observe that the maxima of this average F_t occur when $\alpha = \pi/2$ and its minima are at either $\alpha = 0$ or $\alpha = \pi$. In the same figure (right vertical scale) the experimental values of $\Delta T_c(\alpha)$, for the same cases, which have minima near $\pi/2$, are plotted in an inverted scale. The agreement is truly striking. The anticorrelation can be easily understood: the magnitude of the low-T singlet pair amplitudes is of course positively correlated to T_c. Here the fact that triplet pair amplitudes are anticorrelated to T_c (or to the singlet amplitudes) indicates a singlet-triplet conversion process: when more singlet superconductivity leaks into the ferromagnet side, T_c is suppressed and triplet superconductivity is enhanced. The average magnitude of the triplet pair amplitudes in the free and normal layer regions is only weakly dependent on α: Of importance is the propagation of triplet pairs throughout the entire system, generated by the symmetry-breaking interfaces and magnetic inhomogeneity created from the two misaligned ferromagnets. This clearly demonstrates a singlet to triplet process which is related to the nonmonotonicity of the transition temperature.

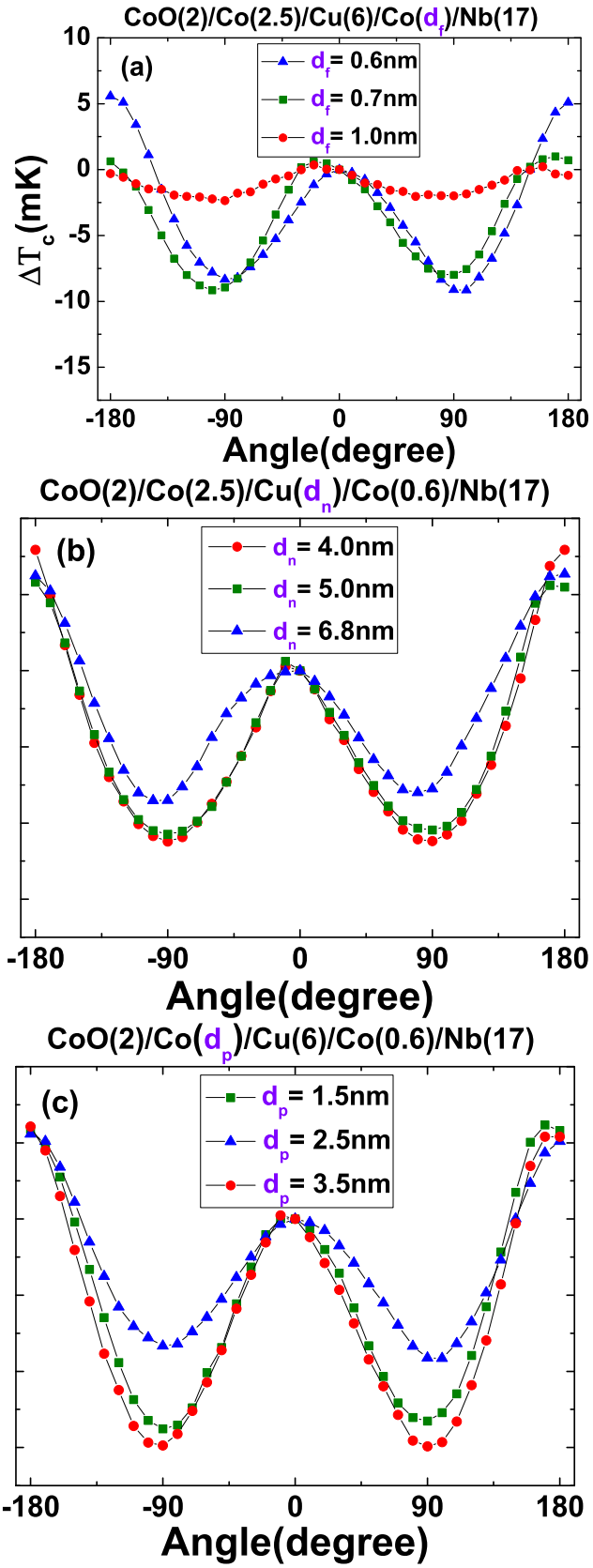

Figure 3.5: $T_c(\alpha)$ for representative samples from the three series of samples studied in this paper. (a) From the d_f series, (b) from the d_n series, (c) from the d_p series.

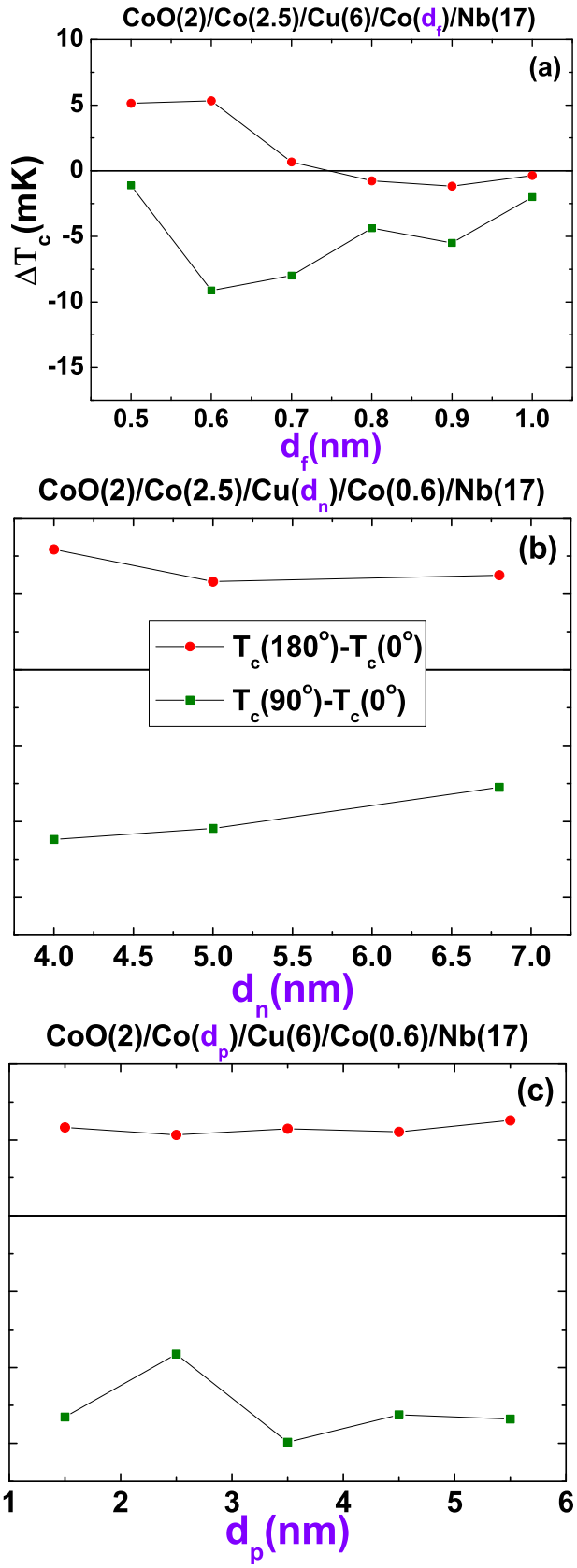

Figure 3.6: Dependence of $T_c(\pi) - T_c(0)$ (red circles) and $T_c(\frac{\pi}{2}) - T_c(0)$ (green squares) on the free Co layer thickness d_f (a), nonmagnetic spacer thickness d_n (b), and pinned layer thickness d_p (c).

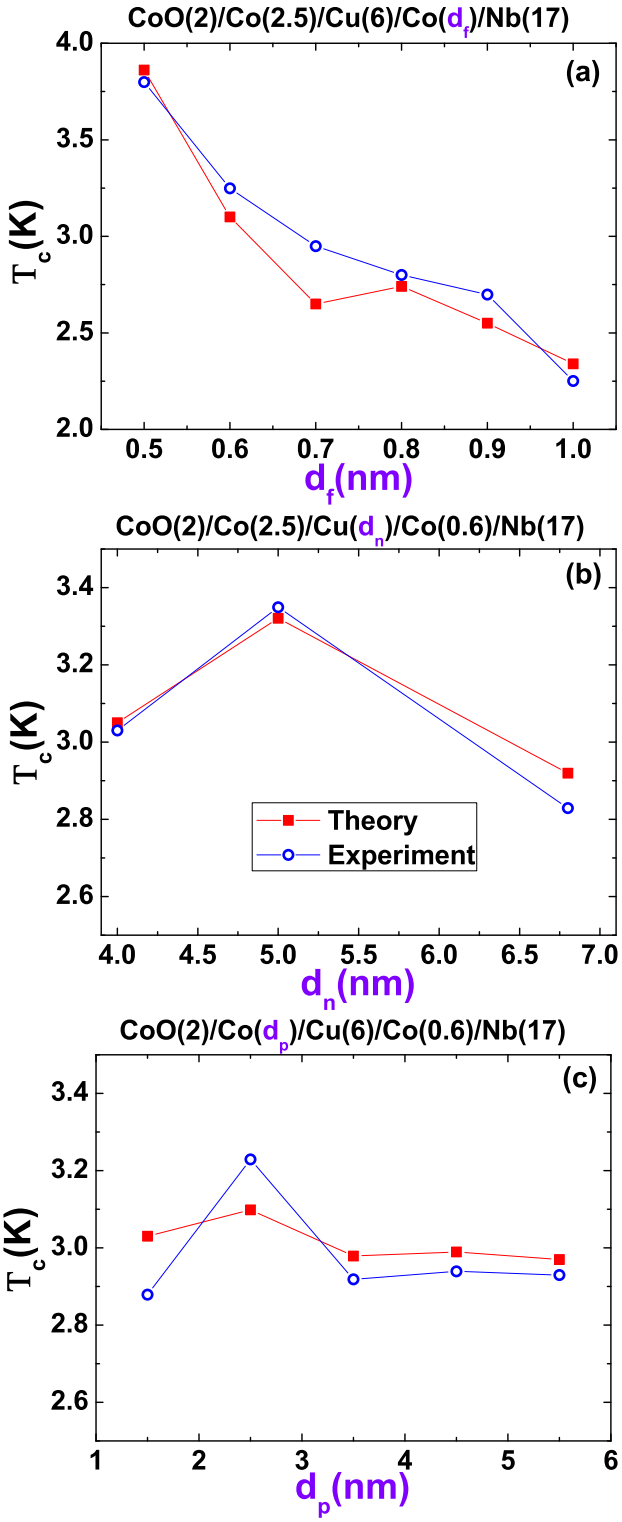

Figure 3.7: Experimental data and theoretical fitting of T_c in the P state as a function of (a) the Co free layer thickness d_f (with $d_n = 6$ nm and $d_p = 2.5$ nm), (b) the Cu normal metal layer thickness d_n (with $d_p = 2.5$ nm and $d_f = 0.6$ nm), and (c) the Co pinned layer thickness d_p (with $d_n = 6$ nm and $d_f = 0.6$ nm).

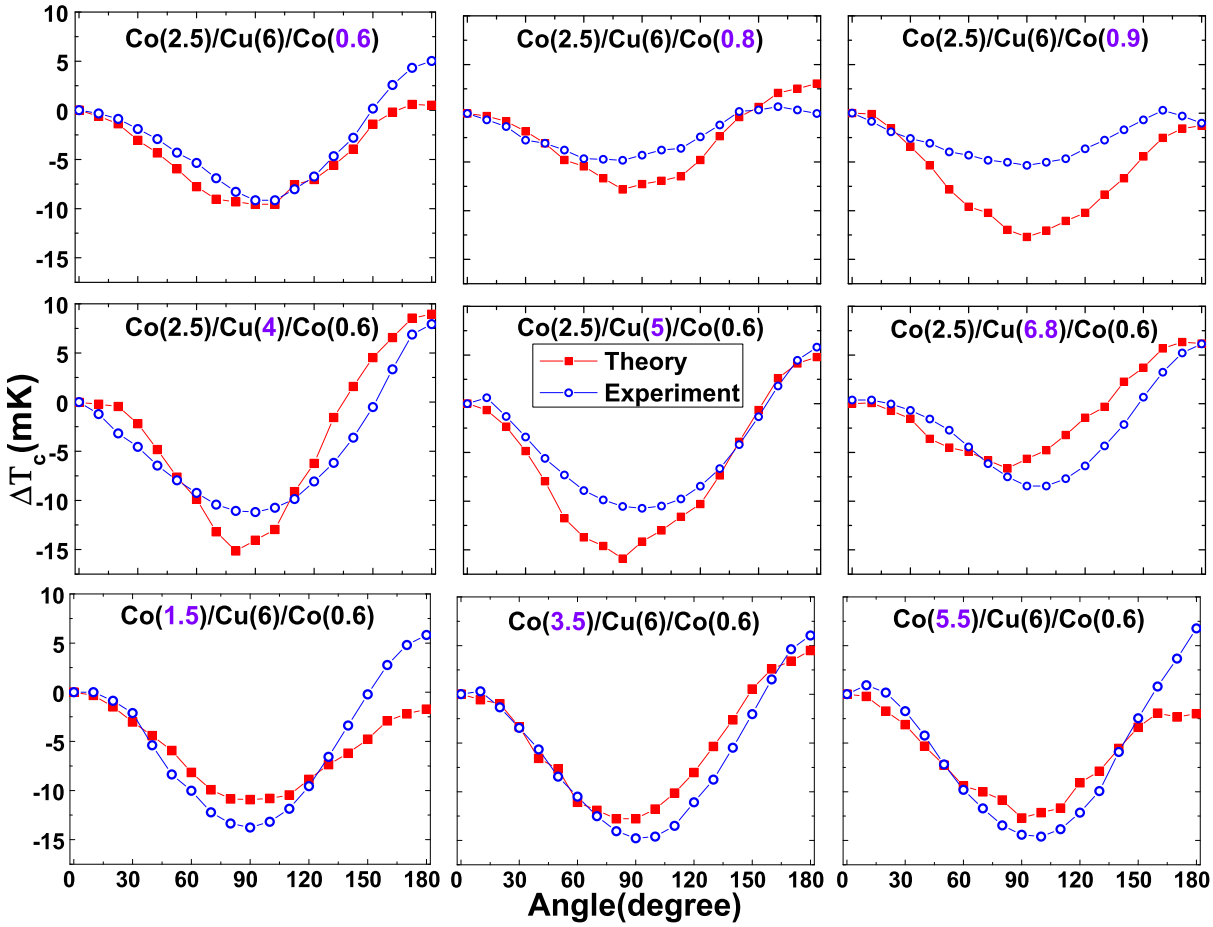

Figure 3.8: Experiment and theory comparisons of ΔT_c [defined as $\Delta T_c(\alpha) \equiv T_c(\alpha) - T_c(0)$] as a function of relative magnetization angle are shown for the three batches of samples. Top row: Three different free layer thicknesses, $d_f = 0.6$ nm, 0.8 nm, 0.9 nm, and with $d_p = 2.5$ nm, $d_n = 6$ nm. Middle row: Three different nonmagnetic layer thicknesses: $d_n = 4$ nm, 5 nm, 6.8 nm, and with $d_f = 0.6$ nm, $d_p = 2.5$ nm. Bottom row: Three different pinned layer thicknesses: $d_p = 1.5$ nm, 3.5 nm, 5.5 nm, and with $d_f = 0.6$ nm, $d_n = 6$ nm.

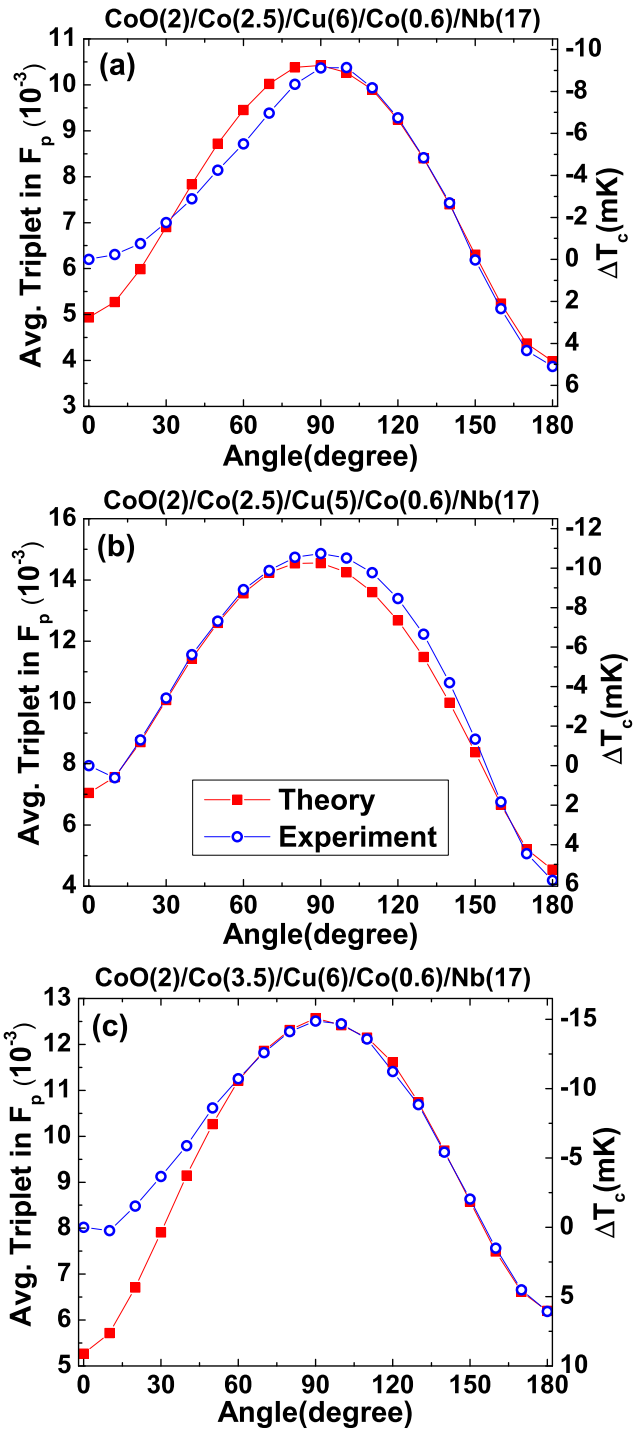

Figure 3.9: Average triplet amplitudes in the pinned ferromagnet layer as a function of relative magnetization angle. The quantity plotted is the average of $F_t(y,t)$ [Eq. (3.8)] in this region, at $\omega_D t = 4$. The quantity ΔT_c is also shown (right scale). Red squares are the theoretical triplet amplitudes (left scale) and the blue circles are the experimental ΔT_c (right inverted scale) as a function of angle. The ΔT_c data correspond to one set chosen from each batch of samples in Fig. 3.8. (a) From the d_f series, (b) from the d_n series, (c) from the d_p series.

Bibliography

[3] L. N. Bulaevski, V. V. Kuzi, and A. A. Sobyanin. *Superconducting system with weak coupling to the current in the ground state*. 1977. URL: http://adsabs.harvard.edu/abs/1977JETPL..25..290B.

[4] A. I. Buzdin, L. N. Bulaevskii, and S. V. Panyukov. "Critical-current oscillations as a function of the exchange field and thickness of the ferromagnetic metal (F) in an S-F-S Josephson junction". In: *JETP Lett.* 35.l (1982), p. 178. URL: http://www.jetpletters.ac.ru/ps/1314/article{_}19853.pdf.

[5] T. Tokuyasu, J. A. Sauls, and D. Rainer. "Proximity effect of a ferromagnetic insulator in contact with a superconductor". In: *Phys. Rev. B* 38.13 (1988), pp. 8823–8833. ISSN: 01631829.

[6] V. V. Ryazanov et al. "Coupling of two superconductors through a ferromagnet: Evidence for a π junction". In: *Phys. Rev. Lett.* 86.11 (2001), pp. 2427–2430. ISSN: 00319007. arXiv: 0008364 [cond-mat].

[7] T Kontos et al. "Josephson Junction through a Thin Ferromagnetic Layer: Negative Coupling". In: *Phys. Rev. Lett.* 89.13 (2002), p. 137007. ISSN: 0031-9007. arXiv: 0201104v2 [cond-mat]. URL: http://link.aps.org/doi/10.1103/PhysRevLett.89.137007.

[8] A. I. Buzdin. "Proximity effects in superconductor-ferromagnet heterostructures". In: *Rev. Mod. Phys.* 77.3 (2005), pp. 935–976. ISSN: 00346861. arXiv: 0505583 [cond-mat].

[9] F. S. Bergeret, A. F. Volkov, and K. B. Efetov. "Odd triplet superconductivity in superconductor ferromagnet structures: A survey". In: *Appl. Phys. A Mater. Sci. Process.* 89.3 (2007), pp. 599–601. ISSN: 09478396. arXiv: 0602522 [cond-mat].

[10] Matthias Eschrig. "Spin-polarized supercurrents for spintronics". In: *Phys. Today* 64.1 (2011), pp. 43–49. ISSN: 00319228. arXiv: 1509.02242.

[11] Klaus Halterman and Oriol T. Valls. "Proximity effects and characteristic lengths in ferromagnet-superconductor structures". In: *Phys. Rev. B* 66.22 (2002), p. 224516. ISSN: 0163-1829. arXiv: 0205518 [cond-mat]. URL: http://arxiv.org/abs/cond-mat/0205518$\backslash$nhttp://link.aps.org/doi/10.1103/PhysRevB.66.224516.

[12] R S Keizer et al. “A spin triplet supercurrent through the half-metallic ferromagnet CrO2.” In: *Nature* 439.7078 (2006), pp. 825–7. ISSN: 1476-4687. arXiv: 0602359 [cond-mat]. URL: http://www.ncbi.nlm.nih.gov/pubmed/16482152.

[13] Jian Wang et al. “Interplay between superconductivity and ferromagnetism in crystalline nanowires”. In: *Nat. Phys.* 6.5 (2010), p. 389. ISSN: 1745-2473. URL: http://dx.doi.org/10.1038/nphys1621.

[14] C. Visani et al. “Equal-spin Andreev reflection and long-range coherent transport in high-temperature superconductor/half-metallic ferromagnet junctions”. In: *Nat. Phys.* 8.7 (2012), pp. 539–543. ISSN: 1745-2473.

[15] F. H{\”u}bler et al. “Observation of Andreev bound states at spin-active interfaces”. In: *Phys. Rev. Lett.* 109.8 (2012), pp. 1–5. ISSN: 00319007. arXiv: 1012.3867.

[16] Klaus Halterman, Paul H. Barsic, and Oriol T. Valls. “Odd triplet pairing in clean superconductor/ferromagnet heterostructures”. In: *Phys. Rev. Lett.* 99.12 (2007), pp. 1–4. ISSN: 00319007. arXiv: 0704.1820.

[17] Klaus Halterman, Oriol T. Valls, and Paul H. Barsic. “Induced triplet pairing in clean s -wave superconductor/ferromagnet layered structures”. In: *Phys. Rev. B - Condens. Matter Mater. Phys.* 77.17 (2008), pp. 1–14. ISSN: 10980121.

[18] Chien-Te Wu, Oriol T. Valls, and Klaus Halterman. “Proximity effects and triplet correlations in ferromagnet/ferromagnet/superconductor nanostructures”. In: *Phys. Rev. B* 86.1 (2012), p. 014523. ISSN: 1098-0121. arXiv: arXiv:1207.1325v1. URL: http://link.aps.org/doi/10.1103/PhysRevB.86.014523.

[19] J W A Robinson, J D S Witt, and M G Blamire. “Controlled Injection of Spin-Triplet Supercurrents into a Strong Ferromagnet”. In: *Science (80-.).* 329.5987 (2010), pp. 59–61. ISSN: 0036-8075, 1095-9203. URL: http://www.sciencemag.org/content/329/5987/59.

[20] Trupti S. Khaire et al. “Observation of spin-triplet superconductivity in co-based josephson junctions”. In: *Phys. Rev. Lett.* 104.13 (2010), pp. 2–5. ISSN: 00319007. arXiv: 0912.0205.

[21] M. S. Anwar et al. “Long range supercurrents in ferromagnetic CrO 2 using a multilayer contact structure”. In: *Appl. Phys. Lett.* 100.5 (2012), pp. 2–5. ISSN: 00036951. arXiv: arXiv:1111.5809v1.

[22] S.D. Gu, J.Y. ; You, C.-Y. ; Jiang, J. S.; Pearson, J.; Bazaliy, Ya. B.; Bader. “Magnetization-Orientation Dependence of the Superconducting Transition Temperature in the Ferromagnet-Superconductor-Ferromagnet System: CuNi=Nb=CuNi”. In: *Phys. Rev. Lett.* 89.15 (2002), p. 157004. ISSN: 0031-9007. URL: http://link.aps.org/doi/10.1103/PhysRevLett.89.157004.

[23] Ion C. Moraru, W. P. Pratt, and Norman O. Birge. “Observation of standard spin-switch effects in ferromagnet/superconductor/ ferromagnet trilayers with a strong ferromagnet”. In: *Phys. Rev. B - Condens. Matter Mater. Phys.* 74.22 (2006), pp. 1–4. ISSN: 10980121.

[24] J. Y. Gu, Jefery Kusnadi, and Chun Yeol You. "Proximity effect in a superconductor/exchange-spring-magnet hybrid system". In: *Phys. Rev. B - Condens. Matter Mater. Phys.* 81.21 (2010), pp. 1–6. ISSN: 10980121.

[25] P. V. Leksin et al. "Evidence for triplet superconductivity in a superconductor-ferromagnet spin valve". In: *Phys. Rev. Lett.* 109.5 (2012), pp. 1–5. ISSN: 00319007. arXiv: arXiv:1207.0727v1.

[26] Yaohua Liu et al. "Effect of interface-induced exchange fields on cuprate-manganite spin switches". In: *Phys. Rev. Lett.* 108.20 (2012), pp. 1–5. ISSN: 00319007. arXiv: 1201.2707.

[27] V. I. Zdravkov et al. "Experimental observation of the triplet spin-valve effect in a superconductor-ferromagnet heterostructure". In: *Phys. Rev. B - Condens. Matter Mater. Phys.* 87.14 (2013), pp. 1–6. ISSN: 10980121.

[28] L. Y. Zhu et al. "Unanticipated proximity behavior in ferromagnet-superconductor heterostructures with controlled magnetic noncollinearity". In: *Phys. Rev. Lett.* 110.17 (2013), pp. 1–5. ISSN: 00319007. arXiv: 1304.6071.

[29] Bin Li et al. "Superconducting spin switch with infinite magnetoresistance induced by an internal exchange field". In: *Phys. Rev. Lett.* 110.9 (2013), pp. 1–5. ISSN: 00319007.

[30] G Nowak, K Westerholt, and H Zabel. "Asymmetric superconducting spin valves based on the Fe/V layer system grown on MgO(100)". In: *Supercond. Sci. Technol.* 26.2 (2013), p. 025004. ISSN: 0953-2048. URL: http://stacks.iop.org/0953-2048/26/i=2/a=025004?key=crossref.1cc6e458e47c52ef6da752e42d1d66a7.

[31] T. Gredig et al. "Rotation of exchange anisotropy in biased Co/CoO bilayers". In: *J. Appl. Phys.* 87.9 III (2000), pp. 6418–6420. ISSN: 00218979.

[32] K. P. Parkin, S. S. P. ; Bhadra, R. ; Roche. "Oscillatory Magnetic Exchange Coupling through Thin Copper Layers". In: *Phys. Rev. Lett.* 66.16 (1991), pp. 2152–2155.

[33] J. Zhu et al. "Origin of the inverse spin switch effect in superconducting spin valves". In: *Phys. Rev. Lett.* 103.2 (2009), pp. 1–4. ISSN: 00319007. arXiv: 0903.0044.

[34] Jian Zhu et al. "Angular dependence of the superconducting transition temperature in ferromagnet-superconductor-ferromagnet trilayers". In: *Phys. Rev. Lett.* 105.20 (2010), pp. 1–4. ISSN: 00319007. arXiv: 1010.1752.

[35] Paul H. Barsic, Oriol T. Valls, and Klaus Halterman. "Thermodynamics and phase diagrams of layered superconductor/ferromagnet nanostructures". In: *Phys. Rev. B - Condens. Matter Mater. Phys.* 75.10 (2007), pp. 1–12. ISSN: 10980121.

[36] F. Chiodi et al. "Supra-oscillatory critical temperature dependence of Nb-Ho bilayers". In: *EPL (Europhysics Lett.* 101.3 (2013), p. 37002. ISSN: 0295-5075. arXiv: arXiv:1211.1169v1. URL: http://stacks.iop.org/0295-5075/101/i=3/a=37002?key=crossref.4541cbc0372719e1539fa2523d56b198.

[37] E. a. Demler, G. B. Arnold, and M. R. Beasley. "Superconducting proximity effects in magnetic metals". In: *Phys. Rev. B* 55.22 (1997), pp. 15174–15182. ISSN: 0163-1829.

[38] Zoran Radovi\'{c} et al. “Transition temperatures of superconductor-ferromagnet superlattices”. In: *Phys. Rev. B* 44.2 (1991), pp. 759–764. ISSN: 01631829.

[39] J. S. Jiang et al. “Oscillatory superconducting transition temperature in Nb/Gd multilayers”. In: *Phys. Rev. Lett.* 74.2 (1995), pp. 314–317. ISSN: 00319007.

[40] Ya. V. Fominov et al. “Superconducting triplet spin valve”. In: *JETP Lett.* 91.6 (2010), pp. 308–313. ISSN: 0021-3640. arXiv: 1002.2113.

[41] T. Yu Karminskaya, A. A. Golubov, and M. Yu Kupriyanov. “Anomalous proximity effect in spin-valve superconductor/ferromagnetic metal/ferromagnetic metal structures”. In: *Phys. Rev. B - Condens. Matter Mater. Phys.* 84.6 (2011), pp. 1–5. ISSN: 10980121.

Chapter 4

Conclusion

In conclusion, this work shows measurements of the superconducting transition temperature T_c in CoO/Co/Cu/Co/Nb multilayers in a spin valve structure. T_c was measured both as a function of the in-plane angle between the Co magnetic moments and of the thicknesses of the Co/Cu/Co spin valve layers. It was found that T_c is a nonmonotonic function of the angle, with a minimum near orthogonal orientations of the magnetic moments of the two Co layers. The behavior of T_c as a function of these variables was quantitatively described by an efficient microscopic method that is based on a linearization of the self-consistent Bogoliubov–de Gennes equations. We have shown that the nonmonotonic behavior of $T_c(\alpha)$ is correlated with the formation of long-range triplet pairs.